

SANDIA REPORT

SAND2013-1159

Unlimited Release

Printed February 2013

Burnup Concept for a Long Life Fast Reactor Core using MCNPX

Thomas V. Holschuh, Edward J. Parma, Tom G. Lewis III

Prepared by
Sandia National Laboratories
Albuquerque, New Mexico 87185 and Livermore, California 94550

Sandia National Laboratories is a multi-program laboratory managed and operated by Sandia Corporation, a wholly owned subsidiary of Lockheed Martin Corporation, for the U.S. Department of Energy's National Nuclear Security Administration under contract DE-AC04-94AL85000.

Approved for public release; further dissemination unlimited.



Sandia National Laboratories



Issued by Sandia National Laboratories, operated for the United States Department of Energy by Sandia Corporation.

NOTICE: This report was prepared as an account of work sponsored by an agency of the United States Government. Neither the United States Government, nor any agency thereof, nor any of their employees, nor any of their contractors, subcontractors, or their employees, make any warranty, express or implied, or assume any legal liability or responsibility for the accuracy, completeness, or usefulness of any information, apparatus, product, or process disclosed, or represent that its use would not infringe privately owned rights. Reference herein to any specific commercial product, process, or service by trade name, trademark, manufacturer, or otherwise, does not necessarily constitute or imply its endorsement, recommendation, or favoring by the United States Government, any agency thereof, or any of their contractors or subcontractors. The views and opinions expressed herein do not necessarily state or reflect those of the United States Government, any agency thereof, or any of their contractors.

Printed in the United States of America. This report has been reproduced directly from the best available copy.

Available to DOE and DOE contractors from
U.S. Department of Energy
Office of Scientific and Technical Information
P.O. Box 62
Oak Ridge, TN 37831

Telephone: (865) 576-8401
Facsimile: (865) 576-5728
E-Mail: reports@adonis.osti.gov
Online ordering: <http://www.osti.gov/bridge>

Available to the public from
U.S. Department of Commerce
National Technical Information Service
5285 Port Royal Rd.
Springfield, VA 22161

Telephone: (800) 553-6847
Facsimile: (703) 605-6900
E-Mail: orders@ntis.fedworld.gov
Online order: <http://www.ntis.gov/help/ordermethods.asp?loc=7-4-0#online>



SAND2013-1159
Unlimited Release
Printed February 2013

Burnup Concept for a Long-Life Fast Reactor Core using MCNPX

Thomas V. Holschuh, Tom G. Lewis III
Advanced Nuclear Concepts

Edward Parma
Applied Nuclear Technologies

Sandia National Laboratories
P.O. Box 5800
Albuquerque, New Mexico 87185-1130

Abstract

This report describes a reactor design with a burnup concept for a long-life fast reactor core that was evaluated using Monte Carlo N-Particle eXtended (MCNPX). The current trend in advanced reactor design is the concept of a small modular reactor (SMR). However, very few of the SMR designs attempt to substantially increase the lifetime of a reactor core, especially without zone loading, fuel reshuffling, or other artificial mechanisms in the core that “flatten” the power profile, including non-uniform cooling, non-uniform moderation, or strategic poison placement. Historically, the limitations of computing capabilities have prevented acceptable margins in the temporal component of the spatial excess reactivity in a reactor design, due primarily to the error in burnup calculations.

This research was performed as an initial scoping analysis into the concept of a long-life fast reactor. It can be shown that a long-life fast reactor concept can be modeled using MCNPX to predict burnup and neutronics behavior. The inherent characteristic of this conceptual design is to minimize the change in reactivity over the lifetime of the reactor. This allows the reactor to operate substantially longer at full power than traditional Light Water Reactors (LWRs) or other SMR designs.

For the purpose of this study, a single core design was investigated: a relatively small reactor core, yielding a medium amount of power (~200 to 400 MW_{th}). The results of this scoping analysis were successful in providing a preliminary reactor design involving metal U-235/U-238 fuel with HT-9 fuel cladding and sodium coolant at a 20% volume fraction.

THIS PAGE INTENTIONALLY LEFT BLANK

CONTENTS

Nomenclature	7
Executive Summary	9
1. Introduction.....	11
2. MCNPX	13
3. k-Infinity Calculations	14
3.1 k_{inf} Geometry.....	14
3.2 MCNPX Tiers	15
3.3 Homogeneous Metal Fuel Mixtures	16
3.4 Oxide Fuel Mixtures	20
3.5 Thorium Mixtures	22
3.6 Second Generation Cores.....	24
3.7 Summary of k_{inf} calculations	26
4. Results of Core Modeling for the LLFR Concept	27
4.1 k_{eff} Geometry.....	27
4.2 Initial Results for MCNPX k_{eff} Calculations for the LLFR Reactor Concept	33
4.3 Core Modifications for LLFR Concept Reactor	38
4.4 Coolant Modifications	41
4.5 Future Generation LLFR Cores	42
5. Conclusions.....	44
6. Future Work	44
7. References.....	45
Appendix A – Sample Input Deck	47
Appendix B – EOL Non-Actinide Isotope Inventory	55
Distribution	57

FIGURES

Figure 1. MCNP k_{inf} geometry used during initial scoping analysis of LLFR concept.....	14
Figure 2. k_{inf} as a function of time to evaluate differences between built-in MCNPX tiers.....	15
Figure 3. U-235/U-238 homogeneous metal mixture.....	17
Figure 4. U-235/U-238 with 10% w Zr homogeneous metal mixture.....	18
Figure 5. U-235/U-238 with 10% w Zr and 15% v Na in a homogeneous metal mixture.....	19
Figure 6. UO_2 (U-235/U-238) Oxide Fuel in a homogenous mixture.....	20
Figure 7. UO_2 (U-235/U-238) Oxide Fuel with 15% v Na in a homogeneous mixture.....	21
Figure 8. U-235/Th-232 homogeneous metal mixture.....	22
Figure 9. U-233/Th-232 homogeneous fuel mixture.....	23
Figure 10. Pu-239/U-238 homogeneous metal mixture.....	24
Figure 11. U-238/Pu-239/25% Pu-240 homogeneous metal mixture.....	25
Figure 12. 2-D image of LLFR geometry used for k_{eff} calculations.....	28
Figure 13. 3-D image of LLFR geometry used for k_{eff} calculations.....	29
Figure 14. Pin geometry for reactor model.....	30
Figure 15. Core pin geometry at the boundary of two fuel regions.....	31
Figure 16. Core pin geometry at the boundary between.....	32
Figure 17. Results for k_{eff} using metal fuel, HT-9 cladding,	33
Figure 18. Results for k_{eff} using metal fuel, HT-9 cladding,	34
Figure 19. β_{eff} as a function of time for LLFR concept reactor	35
Figure 20. Change in reactivity as a function of time for LLFR concept reactor.....	36
Figure 21. Void reactivity worth as a function of time for LLFR concept reactor.....	37
Figure 22. Comparison of relative power levels for LLFR concept reactor.....	38
Figure 23. Core size modifications for 12% enriched LLFR concept	40
Figure 24. Core size modifications for 11.75% enriched LLFR concept.....	41
Figure 25. Coolant modifications 11.75% enriched LLFR concept reactor.....	42
Figure 26. Results of 2nd Generation Core	43

TABLES

Table 1. Optimal Fuel Enrichments for 10-year core lifetime.....	26
Table 2. Parameter modifications	39
Table 3. Reflector alterations for 11.75% enriched core	40
Table 4. Inventory of the 25 Most Abundant Isotopes at end of core lifetime.....	55

NOMENCLATURE

BOL	Beginning of Life
β_{eff}	Delayed Neutron Fraction (Beta-effective)
cf	coolant fraction
DU	depleted Uranium
EBR-I	Experimental Breeder Reactor I
EBR-II	Experimental Breeder Reactor II
ENHS	Encapsulated Nuclear Heat Source
EOL	End of Life
FFTF	Fast Flux Test Facility
k_{eff}	k-effective
k_{inf}	k-infinity
LDRD	Laboratory Directed Research and Development
LLFR	Long Life Fast Reactor
LWR	Light Water Reactor
MCNPX	Monte Carlo n-Particle eXtended
MeV	Mega Electron-volt
MW_{th}	Megawatt-Thermal
MTHM	Metric Ton of Heavy Metal
Na	Sodium
Pb	Lead
PbBi	Lead-Bismuth
Pu	Plutonium
SMR	Small Modular Reactor
Th	Thorium
U	Uranium
UC	Uranium Carbide
UN	Uranium Nitride
UO_2	Uranium Oxide
W/g	Watts/gram
Zr	Zirconium

THIS PAGE INTENTIONALLY LEFT BLANK

EXECUTIVE SUMMARY

This report presents a relatively new transformational reactor concept, designed around the central characteristic of core longevity, that attempts to achieve this principle without using artificial “flattening” mechanisms to create a more uniform power profile for the reactor, such as zone loading or periodic core reshuffling. This long-life fast reactor (LLFR) concept will most likely be applied to a fast spectrum, liquid metal-cooled reactor design, allowing operating lifetime of the core to be extended to more than 10 years at full-power.

The goal of this scoping analysis is to quantify an expected power level, fuel type, and enrichment, as well as to outline a feasible core design, including core size, fuel element size and pitch, and coolant fraction. A parametric approach employed Monte Carlo N-Particle eXtended (MCNPX) to determine isotopic transmutation and burnup within the reactor core as a function of core operating time. A reactor using this LLFR concept as its central design basis provides a large number of benefits over traditional light-water reactor (LWRs) or other small modular reactors (SMRs).

The major advantages of the LLFR concept include the following:

- Long core lifetime;
- Potential long-life 2nd-generation and further generation cores;
- High fuel and actinide burnup;
- Small void reactivity worth from loss of coolant;
- Compact core design;
- Utilization of the fast neutron spectrum;
- Feasible design using today’s technologies;

In the future, a reactor employing the LLFR concept may be characterized by:

- Potential for coupling with advanced power generation systems, such as S-CO₂ Brayton cycle;
- Ability to be fabricated in centrally located manufacturing facility; and
- Potential for use with dry air cooling, allowing for reactor placement far from source of water.

Overall, the LLFR concept as described in this report appears feasible and warrants further examination and study. Additional research is required to increase the resolution of several important issues regarding the reactor and plant design, characterize the distribution of burnup within the core, conduct more refined thermal hydraulic analyses, analyze safety, and verify economic viability.

The research presented in this report was performed under an early career LDRD program granted by Sandia National Laboratories to Tom G. Lewis III concerning SMR design.

THIS PAGE INTENTIONALLY LEFT BLANK

1. INTRODUCTION

The current trend in advanced reactor design is the concept of a small modular reactor (SMR), which is a reduced-size, efficient reactor design that is sized appropriately according to a city's or region's electrical grid requirements. Currently, large (3000 MWth) light water reactors (LWRs) cost several billion dollars, as well as many years to construct and license. SMRs aim to reduce the initial costs of a nuclear reactor by several orders of magnitude. However, very few of the SMR designs attempt to substantially increase the lifetime of a reactor core, especially without zone loading or other artificial mechanisms in the core that "flatten" the power profile, including non-uniform cooling, non-uniform moderation, or strategic poison placement.

The long life fast reactor (LLFR) is a revolutionary reactor concept for electrical power generation and potential actinide burning, increasing core lifetime to approximately 10-20 years. The LLFR also provides a reduction in the inventory of long-lived actinides, which are major contributors to high-level waste after fuel consumption. Actinides are the major contributor to the long-term heat load and radiotoxicity of repositories, thus any decrease in their inventory can be directly applicable to a safer and cheaper repository scheme. The goal of this scoping analysis was to quantify an expected power level, fuel type, and enrichment, as well as to outline a feasible core design, including core size, fuel element size and pitch, and coolant fraction. A parametric approach employed Monte Carlo N-Particle eXtended (MCNPX) to determine isotopic transmutation and burnup within the reactor core as a function of core operating time, as well as to predict burnup and neutronics behavior. A variety of MCNPX options was assessed to fully model the phenomena that occur in this type of reactor. The inherent characteristic of this design is to minimize the change in reactivity across the lifetime of the reactor. This allows the reactor to operate substantially longer than traditional LWRs or other SMR designs.

A parametric approach employed MCNPX to determine isotopic transmutation and burnup within the reactor core as a function of core operating time. A reactor utilizing this LLFR concept as its central design basis provides a large number of benefits over LWRs or other SMRs. The major advantages of the concept include the following:

- Long core lifetime;
- Potential long-life 2nd-generation and further generation cores;
- High fuel and actinide burnup;
- Small void reactivity worth from loss of coolant;
- Compact core design;
- Utilization of the fast neutron spectrum;
- Feasible design using today's technologies;
- Potential for coupling with advanced power generation systems, such as S-CO₂ Brayton cycle (Parma, et al, 2011);
- Ability to be fabricated in centrally located manufacturing facility; and
- Potential for use with dry air cooling, allowing for reactor placement far from source of water.

This analysis began by first performing k-infinity (k_{inf}) calculations to determine fuel type/enrichment arrangements that effectively display a low-change in k_{inf} over the life of a reactor core. Using enrichment levels deemed eligible by k_{inf} calculations, a full-size fast reactor core could then be evaluated in further MCNPX cases. A single core design was investigated for the purpose of this study. This kind of reactor core is relatively small, yielding a medium amount of power (~200 to 400 MW_{th}).

2. MCNPX

MCNPX (MCNPX, 2011) is a general purpose Monte Carlo radiation transport code designed to track many particle types over a broad range of energies. It is the current generation of a series of Monte Carlo transport codes that began at Los Alamos National Laboratory nearly sixty years ago.

The current version of MCNPX contains new physics subroutines and packages that allow for modeling of phenomena associated with fuel burnup and depletion. One of the unique features of MCNPX includes the ability to potentially track of hundreds of fission products, with the user being able to select isotopes either by specifying pre-defined tiers, as will be discussed later, or by creating a custom isotope list. This burnup package is called through the “Burn” card. The “Burn” card allows the user to define power level, duration, and burnable materials, as well as additional options. The “Burn” card was utilized extensively during this scoping analysis to effectively calculate burnup without implementing an external, custom FORTRAN ode (Parma, 2002). MCNPX obtains its burn, or depletion, capability through the use of CINDER90, a transmutation code used extensively in nuclear research. MCNPX performs individual criticality calculations for each time step indicated by the user within the “Burn” card of the input deck. However, between each time step, CINDER90 executes its own program, altering isotopes based on the neutron interaction rate in the criticality calculation. This sequence allows for an accurate long-term reactivity calculation, an ideal characteristic for the analysis described in this report.

One of the most important features of the “Burn” card is the three built-in “tiers” of fission products available to the user. The three tiers have an increasing number of fission products, ranging from the 12 most common fission products in Tier 1, to 87 and 220 fission products in Tier 2 and Tier 3, respectively. The user also has the ability to add isotopes to any selected tier to customize the burnup calculation. For this analysis, ENDF/VII cross sections were used, operating with coolant, fuel cladding, and fuel temperatures at 600K, 900K, and 1200K, respectively.

To effectively confirm the MCNPX calculations, a similar, compatible Monte Carlo code, MCNP5 (MCNP, 2003), was also employed for β_{eff} and individual step criticality calculations, because MCNP5 is incapable of performing full-scale burnup runs. In a further expansion of this research, an additional criticality and burnup confirmation may be performed using other transmutation codes.

3. K-INFINITY CALCULATIONS

The entire concept of an LLFR originates with an attempt to minimize the change of reactivity over the lifetime of the reactor. No extensive research has been found that attempts to keep the multiplication factor at the same value for ten years or more. In order to determine the proper enrichment for a full-size commercial reactor, calculations were performed using MCNPX that modeled a single fuel element with specular reflectors, simulating an infinite fuel lattice. For each fuel type, several different enrichments were evaluated to comparatively determine an optimal value. Any enrichments that do not display a desirable slope for the multiplication constant, as depicted in figures further in this section, are disregarded for future consideration as part of the full-size reactor MCNPX cases.

To determine the appropriate enrichment range for a long-life reactor core, initial burnup calculations were performed for an infinite reactor system.

3.1 k_{inf} Geometry

All k_{inf} cases were run using the same geometry, and were burned at 50 W/g ($MW_{th}/MTHM$) of fuel, a conservative, typical value for fast reactors (Chang 2006), for a period of 20 years without refueling or rearrangement of fuel. Figure 1 displays the fuel piece modeled in the MCNPX k_{inf} cases. The cylindrical cell has a diameter of 20 centimeters with a height of 40 centimeters. All surfaces are denoted as reflecting within MCNPX to eliminate the leakage of any neutrons.

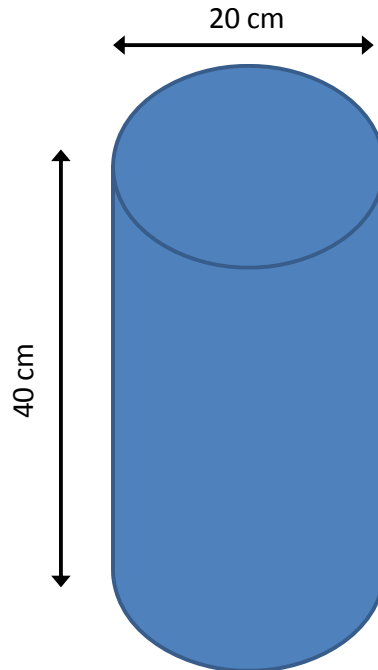


Figure 1. MCNP k_{inf} geometry used during initial scoping analysis of LLFR concept.

3.2 MCNPX Tiers

The initial step when utilizing the MCNPX “Burn” card is to distinguish which options in the card are required, because each option that is unnecessarily included will waste computational time. One of the most important factors in the transmutation of any material is the availability of daughter nuclides and decay products. The tiers available in MCNPX were evaluated to determine the differences in criticality that existed between each tier, based on the substantial difference in available isotopes. A homogeneous metal mixture of U-235 and U-238, enriched to 12%, was used as a test case, because previous research (Kim 2010) indicated that a fast reactor core of approximately this enrichment would display desired characteristics. Figure 2 displays the results of the evaluation of these tiers.

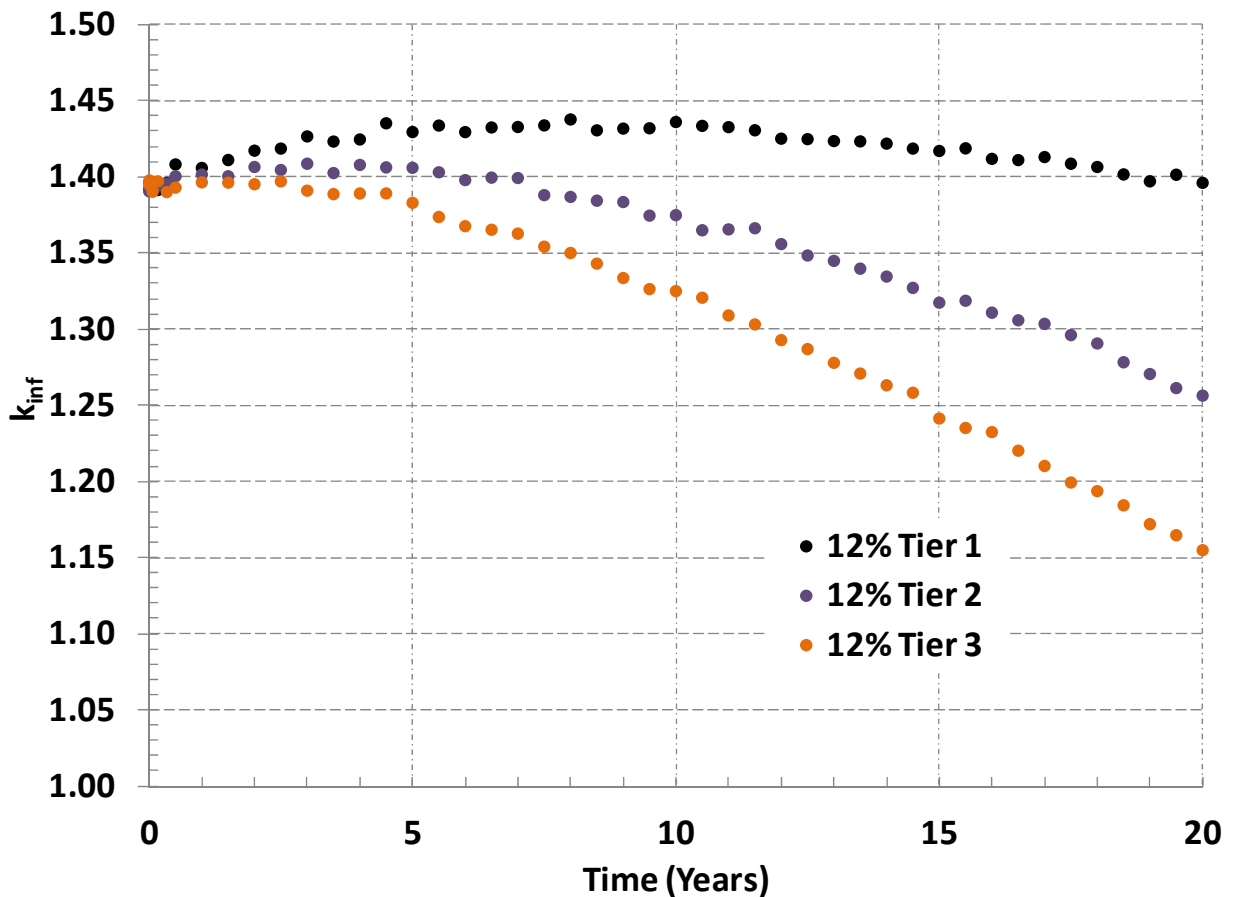


Figure 2. k_{inf} as a function of time to evaluate differences between built-in MCNPX tiers.

In Figure 2, the Tier 1 test case shows an extremely small change in reactivity from the first time step to the conclusion of the test. However, as a result of the data represented in Figure 2, it was deemed necessary to include the Tier 3 fission products, because the disparity between the k_{inf} values from only including Tier 1 and Tier 2 was demonstrated to be readily apparent and non-negligible. Unfortunately, this substantially increases computational time due to the inclusion of hundreds of fission products, but Figure 2 indicates that it is necessary to include Tier 3 fission products to obtain an accurate solution for all future calculations.

3.3 Homogeneous Metal Fuel Mixtures

To assess many types of reactor designs, it is essential to choose a fuel type for the LLFR concept. Many fuel options were evaluated using this k_{inf} method. Figure 3 shows the results for this k_{inf} evaluation using a homogeneous mixture of U-235 and U-238. In the legend, the percentages represent the enrichment ratio of U-235 to U-238 in the mixture. It is important to recall that the goal of the LLFR concept is to find an enrichment that provides the smallest change in reactivity over time. A minimal change in reactivity results from a balance of production and depletion of fissionable isotopes within the core. For example, when a reactor core is designed for enriched U-235, there is also U-238 present in the fuel. At the same time that U-235 is being used, U-238 isotopes are being converted to Pu-239 by neutron capture and beta decay mechanisms. On Figure 3, it is important to note that the k_{inf} for all enrichments converges together as operating time is increased for each test case. This occurs due to the fact that each test case contains equivalent concentrations of fissionable isotopes at specific time steps, since a reactor core that begins with a low enrichment of U-235 produces more fissionable Pu-239 due to the increased abundance of U-238.

For all figures that illustrate a k_{inf} value as a function of time, there is an optimal duration for reactor operations and optimal enrichment, because all k_{inf} values will decrease below unity as time increases to infinity. The optimum enrichment for all cases is summarized in section 3.7.

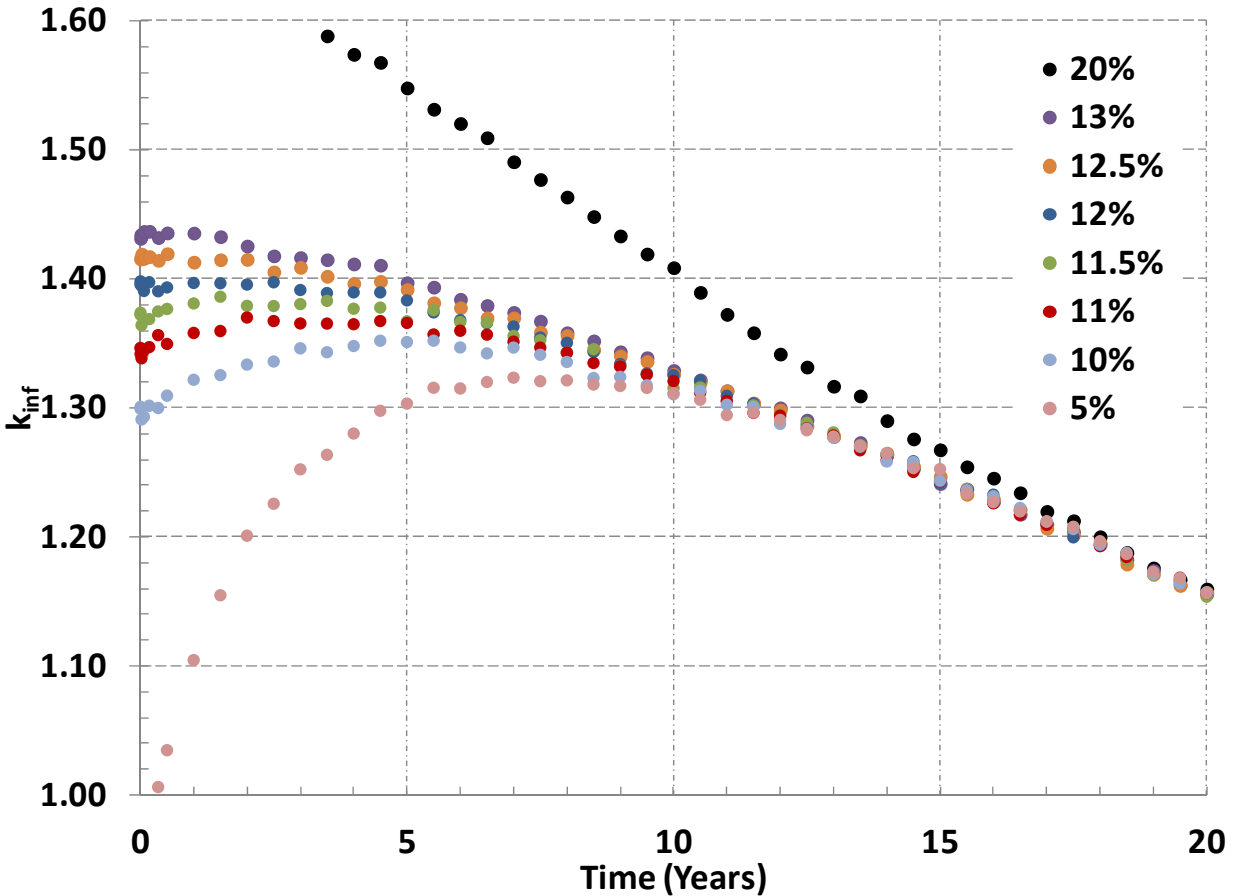


Figure 3. U-235/U-238 homogeneous metal mixture.

Although Figure 3 provides an initial look into the LLFR concept, a commercial reactor does not consist of a homogeneous fuel mixture. Fuel cladding and a coolant material supply are additional variables that must be accounted for in the k_{inf} analysis. Because this k_{inf} analysis is intended to be an approximation, Figure 3 provides an acceptable range, rather than an exact enrichment for full size reactor core simulations to be performed in the future. From Figure 3, it appears that the profiles for 11% or 11.5% enriched cores stay flat for about 7 years. However, for evaluation of a full-size reactor, a range of enrichments from 11% to 13% could produce an acceptable LLFR core.

Figure 4 and Figure 5 include the complete metal fuel mixture and fuel plus coolant, respectively. The metal fuel mixture was approximated to by adding natural Zirconium (Zr), added at 10% by weight into the homogenous mixture geometry of Figure 1. The 10% by weight of Zr was chosen, because it is a typical value for the weight ratio between Zr and heavy metal within a fuel rod for fast reactors, similar to the driver fuel used in the Experimental Breeder Reactor II (EBR-II) at Idaho National Laboratory (Bays 2009).

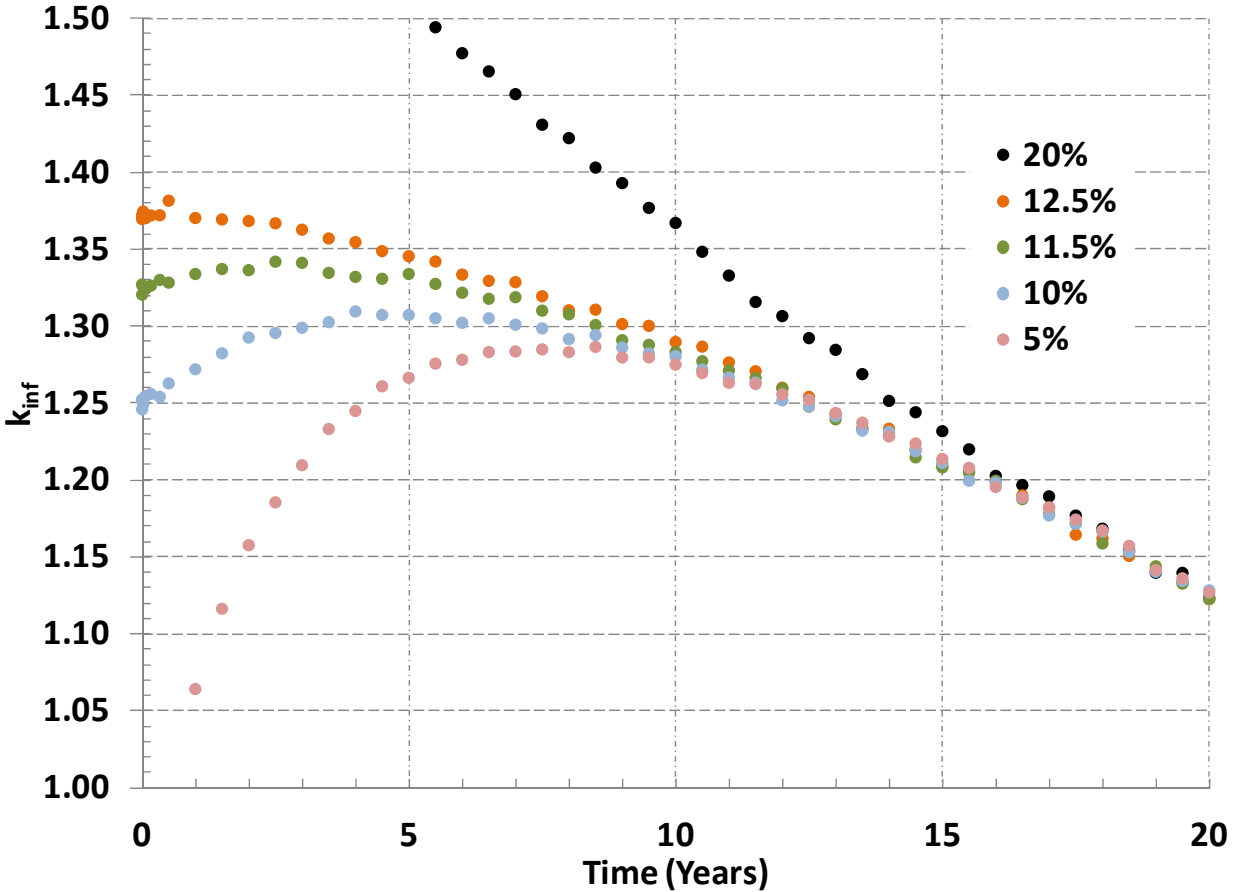


Figure 4. U-235/U-238 with 10%w Zr homogeneous metal mixture.

As compared with Figure 3, Figure 4 displays slightly lower values for k_{inf} , since introducing atoms with a smaller mass (Zr) alters the average neutron energy, since collisions with the Zr results in a lower neutron energy than collisions with heavier atoms. The neutron energy has a direct result on the value of η , the amount of neutrons released per absorption, for U-235, as well as its σ_f (fission cross section) value.

Any future reactor that utilizes the LLFR concept will most likely have a high core power density, making a liquid metal the most logical moderator and coolant choice. As part of this k_{inf} analysis, liquid sodium (Na) was chosen as the coolant, typical for a relatively small fast reactor. So, Figure 5 exhibits a series of k_{inf} cases that contain 15% Na by volume in addition to the U-235, U-238, and Zr already contained in the mixture.

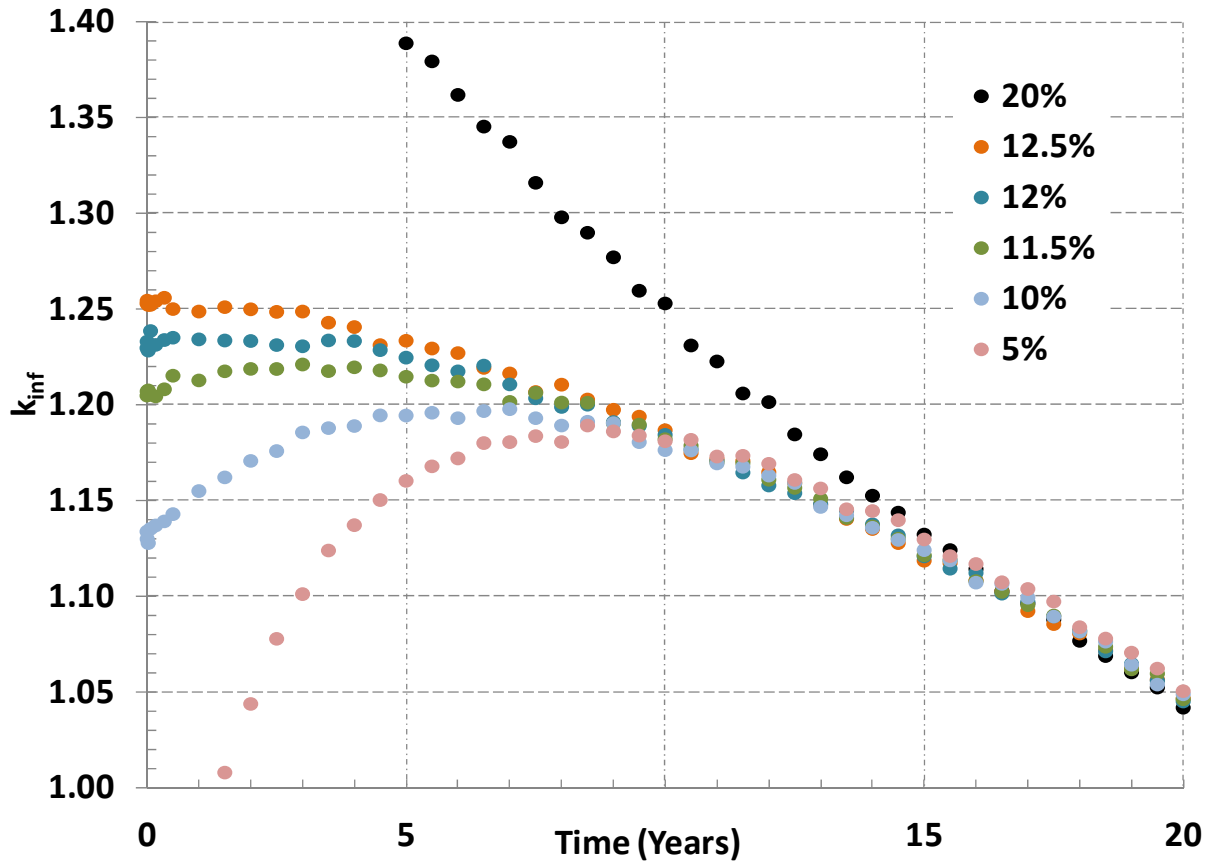


Figure 5. U-235/U-238 with 10%w Zr and 15%v Na in a homogeneous metal mixture.

As compared with Figure 4, the k_{inf} cases are “flatter” for select values of enrichment in Figure 5, as well as providing a decreased value. Once again, this is due to the shifting neutron energy spectrum as a result of the inclusion of sodium atoms, which are lighter than zirconium or uranium isotopes and decrease the neutron energy further.

3.4 Oxide Fuel Mixtures

Figure 3, Figure 4, and Figure 5 provide speculation for a LLFR-concept reactor that would operate with metal fuel. However, this study would be remiss if oxide fuel was not included within the k_{inf} scoping analysis. Figure 6 presents the case results for UO_2 fuel, with the percentage in the legend representing the enrichment ratio of U-235 to U-238.

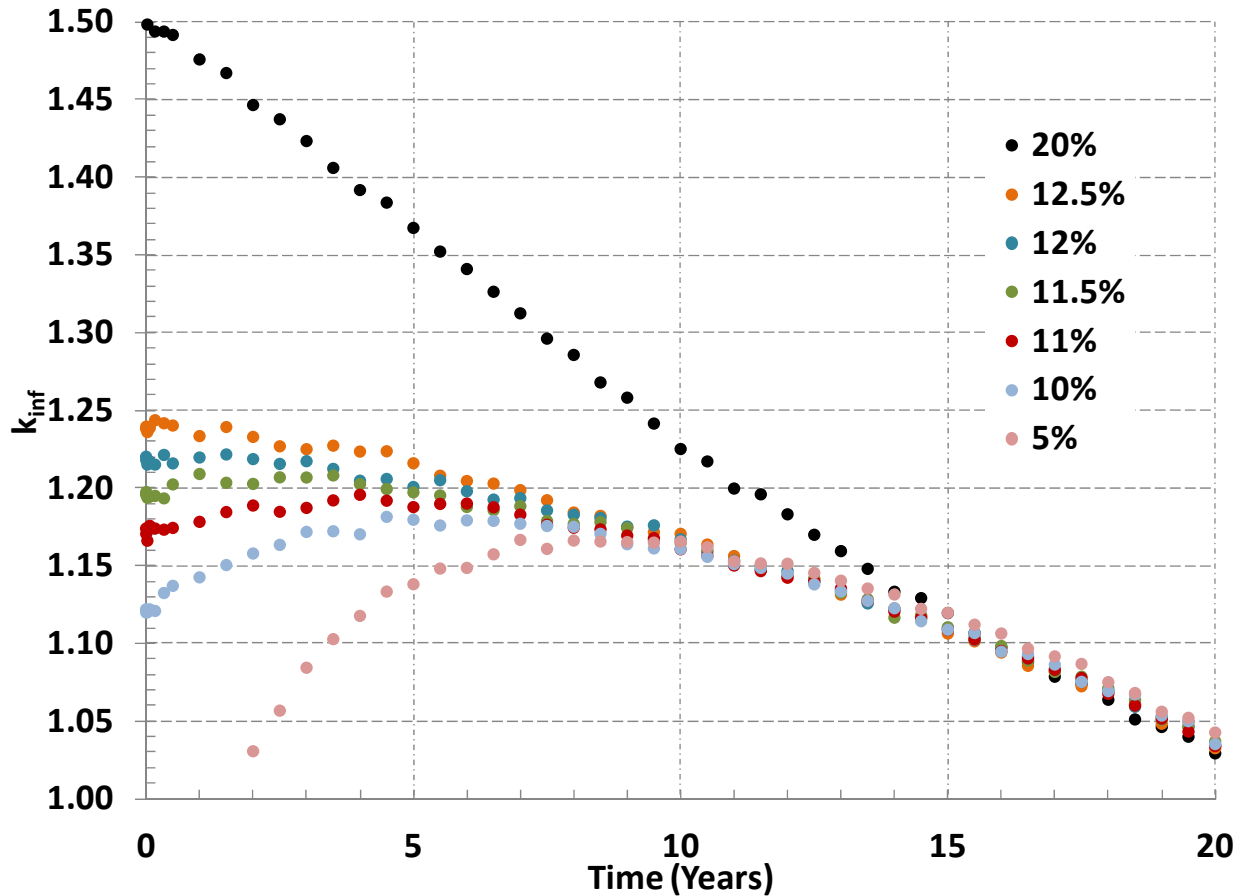


Figure 6. UO_2 (U-235/U-238) Oxide Fuel in a homogenous mixture.

For the oxide fuel case in Figure 6, a further investigation was performed to include 15% Na by volume for the coolant. These results are shown in Figure 7.

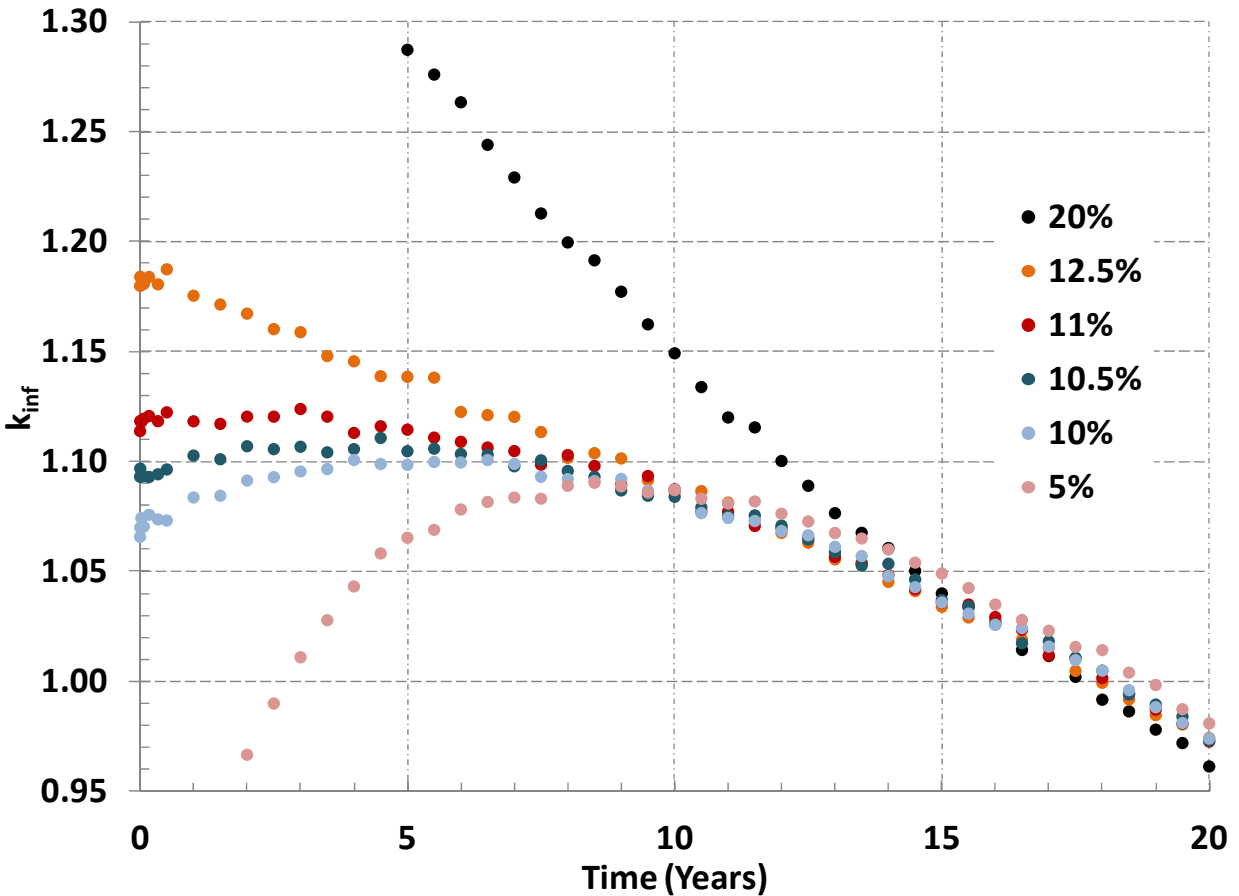


Figure 7. UO₂ (U-235/U-238) Oxide Fuel with 15%v Na in a homogeneous mixture.

The k_{inf} trend displayed in Figure 7 is very similar to Figure 6, despite the slightly decreased value. In both the oxide and metal fuel cases, the included sodium coolant seems to have a stabilizing effect on the criticality of the homogeneous mixture, at least until the case has reached a period of approximately 10 years. This would indicate that for the given average neutron energy in a core with this atomic composition, the values of η for Pu-239 and U-235 are very nearly the same.

3.5 Thorium Mixtures

Following the evaluation of the oxide and metal fuel cases, less widely-used fuel mixtures were evaluated. Figure 8 shows the results of a k_{inf} case consisting of a homogeneous mixture of U-235 and thorium (Th-232). In this case, the Th-232 is included as the fertile material, producing fissionable U-233 through transmutation. The percentage in the legend of Figure 8 represents the enrichment percentage of U-235, as compared to the bulk mass of thorium.

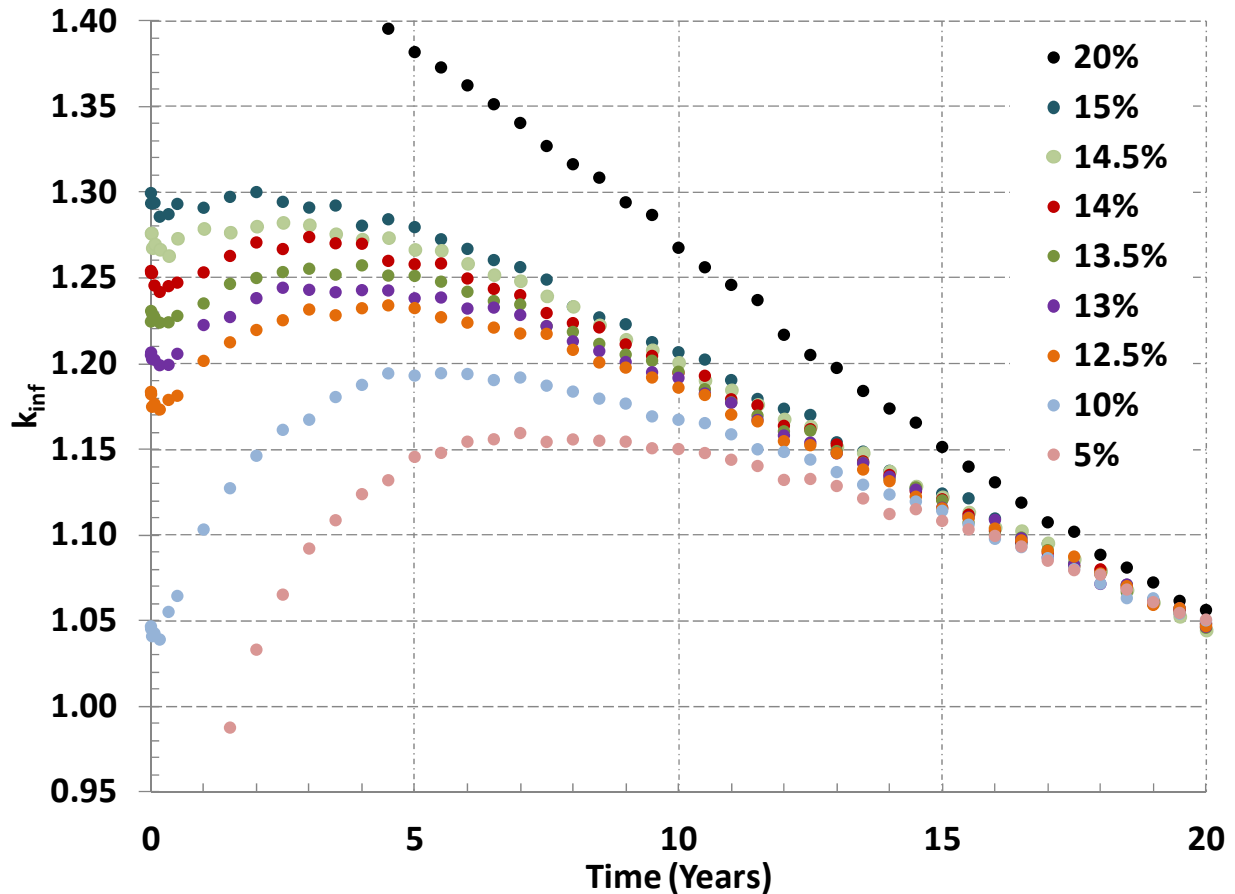


Figure 8. U-235/Th-232 homogeneous metal mixture.

The shape and enrichment in Figure 8 are also similar to the oxide and metal fuels described in previous figures. However, an initial decrease in k_{inf} is visible for each case, due to the production of Protactinium-233 (Pa-233) following Th-232 absorption and Th-233 beta decay ($t_{1/2} = 21.83$ min). Pa-233 has a 22 day half life, so there is a delay between the production of neutrons from fission of U-235 to the production of U-233. Following the initial decrease, there is a sharper increase of reactivity when compared to the metal and oxide cases due to the difference in fissionable isotopes as compared to previous test cases that used U-238 as the fertile material.

Figure 9 addresses the effect of initializing the fuel cycle with U-233 and thorium, rather than using U-235 as the introductory fissionable material. The percentage in the legend of Figure 9 represents the enrichment of U-233 as compared to Th-232.

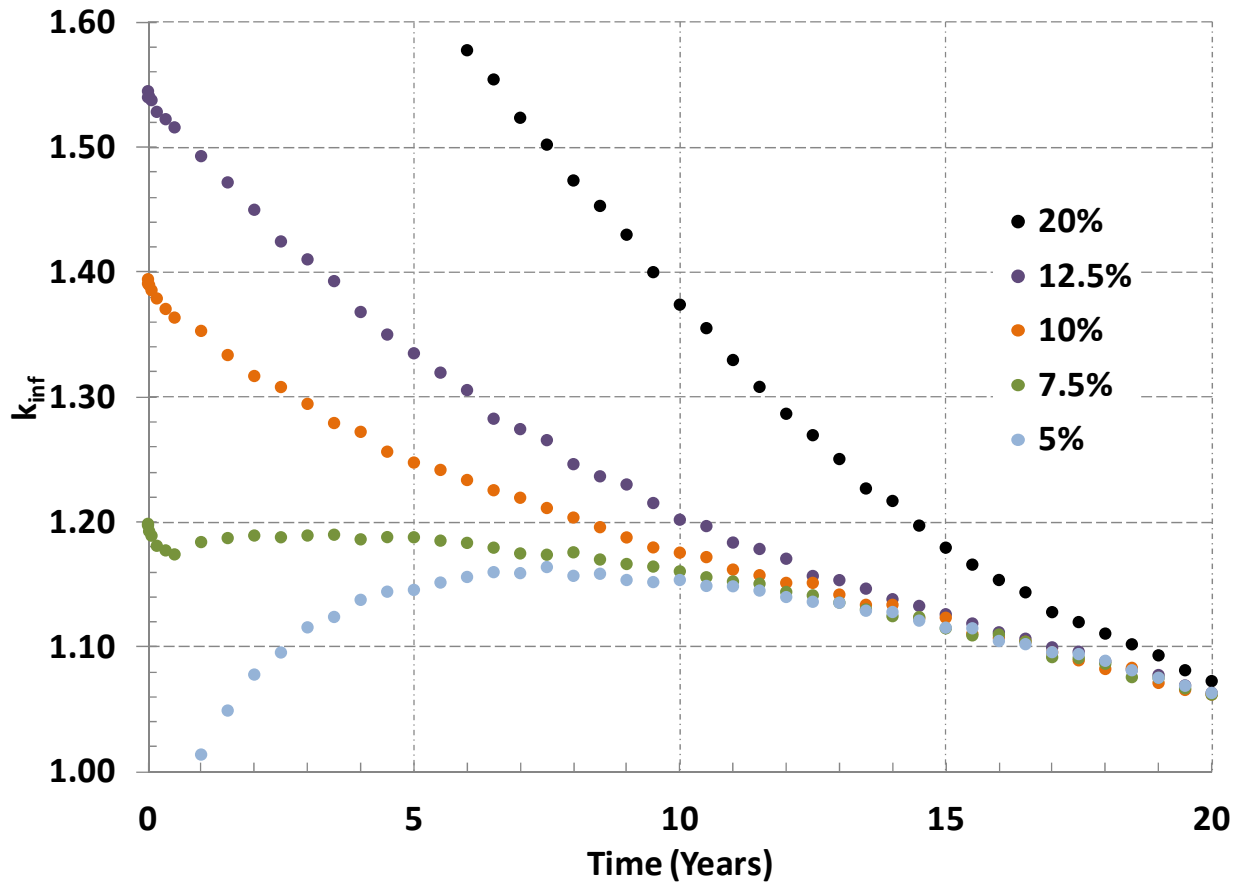


Figure 9. U-233/Th-232 homogeneous fuel mixture.

The “flattest” profile in set of cases illustrated in Figure 9 is at a considerably lower enrichment percentage than the oxide or metal fuel cases, due to the increased η and σ_f values for U-233 with high energy neutrons. Also, in Figure 9, an initial rise in reactivity is avoided, because the fresh fuel contains U-233, rather than U-235. Therefore, the fissionable isotopes bred from the fertile material would be identical to the fissionable isotopes present at beginning of life (BOL), rather than the transition shown in previous cases in which the dominant fuel was converted from U-235 to Pu-239.

3.6 Second Generation Cores

One of the additional goals of the LLFR concept is to be able to run multiple reactor cores using only a single starting core enrichment. To accomplish this, at the end of the first core's lifetime (10-20 years) the fuel will be reprocessed by purging the fuel material of fission products only, and retaining all actinides for the second generation of the core. Depleted uranium (~0.2% enriched) will be added to the second core to replace the mass lost when fission products are removed from the fuel. To model these second cores as part of the k_{inf} analysis, plutonium (Pu) is introduced into the homogeneous mixture.

Figure 10 illustrates the effect of introducing plutonium into the geometry. The percentage in the legend represents the enrichment of Pu-239 with respect to U-238.

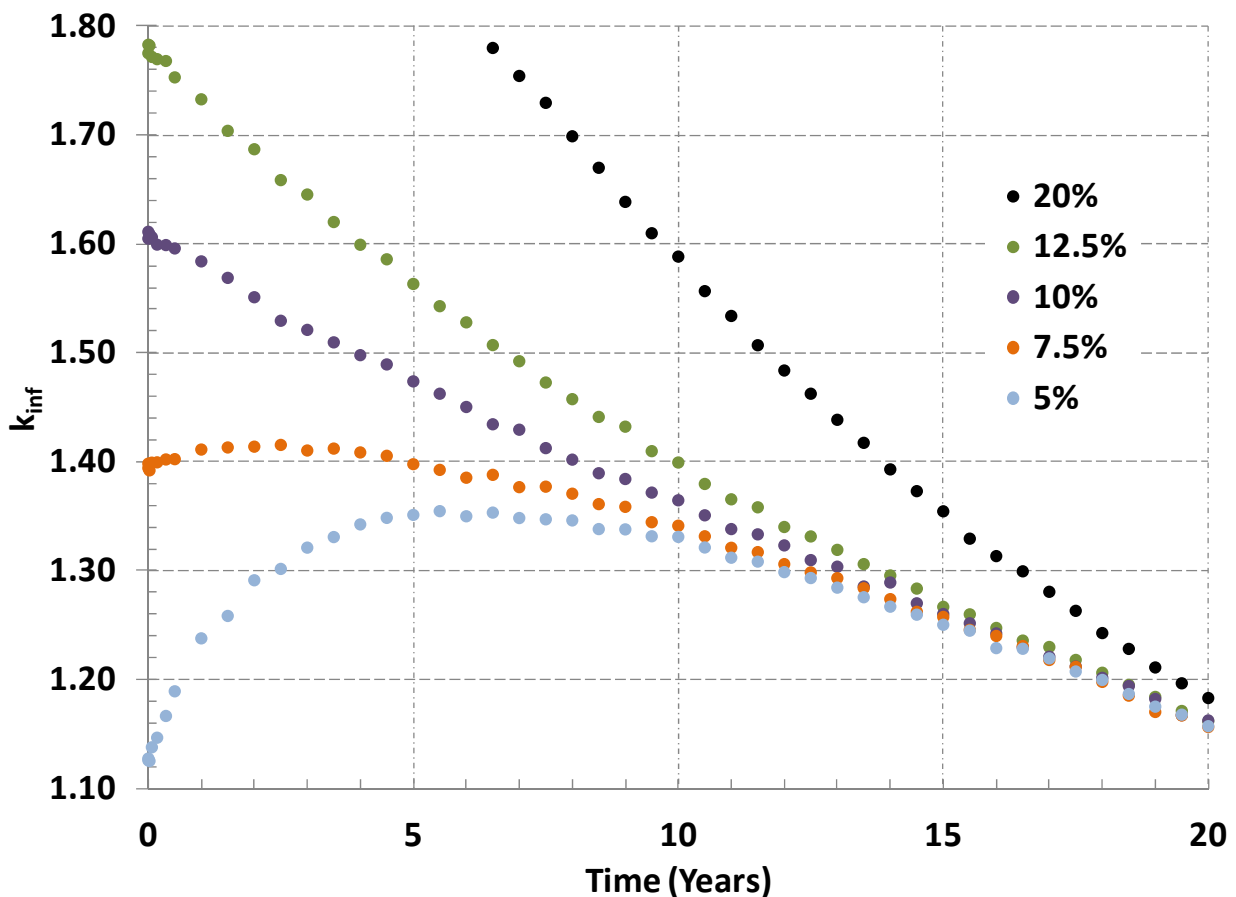


Figure 10. Pu-239/U-238 homogeneous metal mixture.

Figure 10 shows that a smaller enrichment is needed for this mixture than with U-235-initiated metal or oxide fuel, due to the increased η and σ_f values for Pu-239 with high energy neutrons, as compared to U-235.

However, non-fissionable isotopes of plutonium (Pu-240, Pu-242) will also be produced in the initial core, which could become major factors that affect the criticality of the second generation core. As a nominal value, it was assumed that approximately 25% of the plutonium isotopes produced in the initial core would be non-fissionable plutonium. Usually a fast reactor produces a smaller percentage of non-fissionable plutonium isotopes, but 25% was chosen as a conservative, over-estimating value (DeHart, 2010). Figure 11 displays the k_{inf} calculation, including the 25% Pu-240.

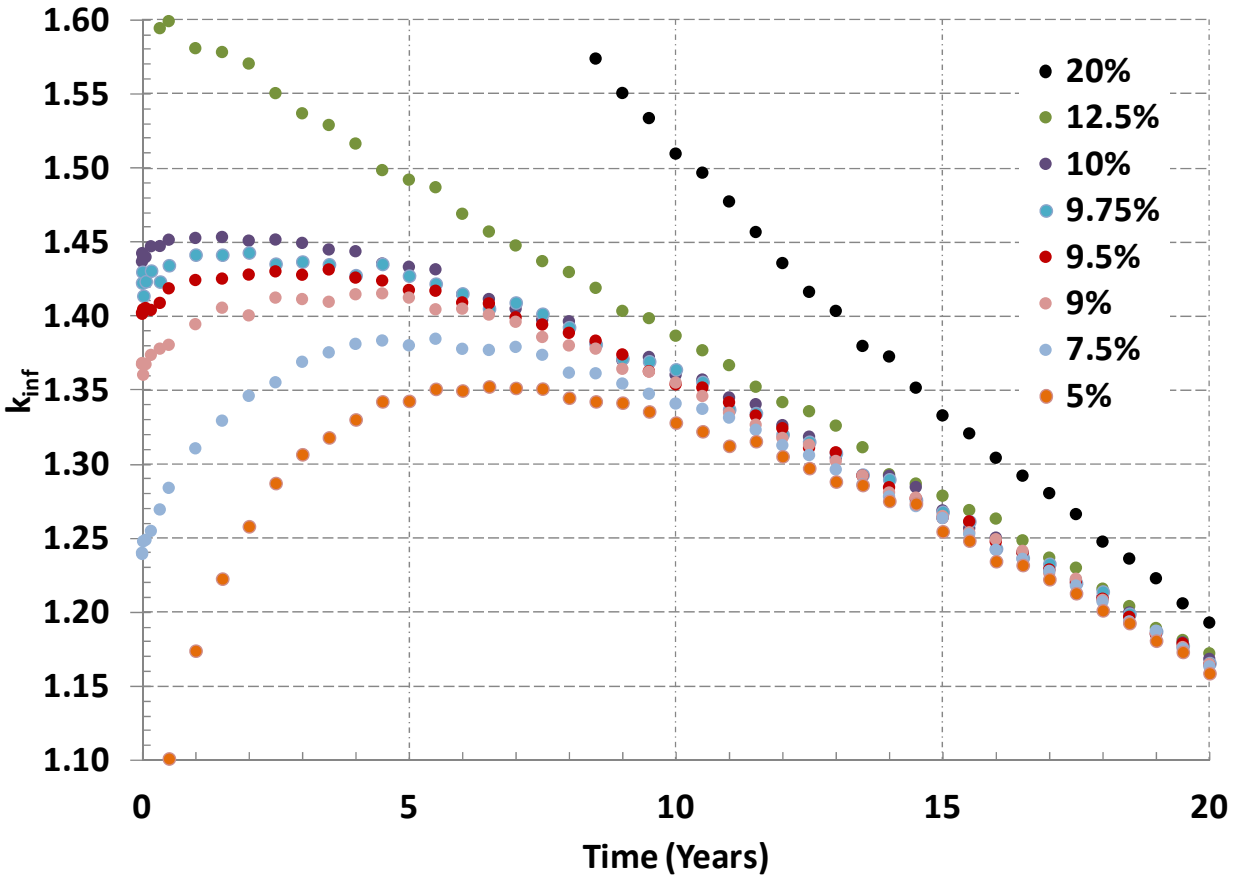


Figure 11. U-238/Pu-239/25% Pu-240 homogeneous metal mixture.

Observe that Figure 10 and Figure 11 possess similar profile shapes, though the similarities occur with different enrichment percentages. This is due to the negative reactivity associated with the higher neutron capture rates of the non-fissionable isotopes of plutonium. To compensate for this phenomenon, more fissionable plutonium must be included within the homogeneous mixture to maintain an ideal long-life k_{inf} profile.

3.7 Summary of k_{inf} calculations

Table 1 provides a matrix of the k_{inf} runs that were performed using MCNPX for the different fuel types, and for the optimal enrichment for the fuel types examined. The “optimal enrichment” in the table represents the enrichment that depicts the “flattest” profile for approximately 10 years of operating time.

Table 1. Optimal Fuel Enrichments for 10-year core lifetime for each set of Fuel Materials run in MCNPX cases.

Fuel Element Materials	Optimal Enrichment
Metal Fuel (U-238, U-235)	12%
Metal Fuel (U-238, U-235, 10% wZr)	11.5%
Metal Fuel (U-238, U-235, 15% vNa, 10% wZr)	12%
Oxide Fuel (U-235, U-238)	11.5%
Oxide Fuel (U-235, U-238, 15% vNa)	11%
Metal Fuel (Th-232, U-233)	7.5%
Metal Fuel (Th-232, U-235)	14.5%
Metal Fuel (U-238, Pu-239)	7.5%
Metal Fuel (U-238, Pu-239, 25% Pu-240)	9.75%

These results can be used as a starting point for a full-scale core modeling analysis. For example, based on Table 1, the enrichment for U-235, U-238 metal, 10% w Zr, and 15% v Na should be approximately between 11% and 13%. This would represent initial enrichment values for a reactor with metal fuel and sodium coolant fraction of 15%. The next section will address the strategies, parameterization, and results of a full-scale reactor analysis using MCNPX.

4. RESULTS OF CORE MODELING FOR THE LLFR CONCEPT

It can be shown that an LLFR concept core can be created that exhibits a steady k_{eff} vs. time profile for 10+ years, taking into account the negative reactivity associated with accumulating fission products. No zone loading, periodic core reshuffling, or other artificial mechanisms are required for this steady k_{eff} profile. Several existing SMR designs claim a long-life core, such as the Encapsulated Nuclear Heat Source (ENHS) (Greenspan 2003), but each differs by one or more important design aspects from the LLFR concept. For the full core modeling, the fuel uses cross-sections based on appropriate temperatures for a fast reactor design: fuel at 1200K, cladding at 900K, and coolant at 600K.

4.1 k_{eff} Geometry

The core design chosen from the previous k_{inf} runs to be initially evaluated for a full-size design was a U-235/U-238/10%w Zr metal fuel, a 20% sodium coolant fraction (cf), and enrichments ranging from 11.5% to 13% at a power level of 400 MW_{th}, to allow for a long core lifetime. Other fuel compositions were discarded for requiring either Pu-239 or U-233 to fuel the initial LLFR core, since material would have needed to be acquired from other reactor sources. The cladding chosen for this analysis was HT-9, a typical high temperature steel cladding with relatively high percentages of chromium detailed by Klueh and Harries (2001), Crawford, et al (2007), and Walters, et al (2011). This cladding material has been tested in several sodium fast experimental reactors, including the Experimental Breeder Reactor I and II (EBR-I and EBR-II) and the Fast Flux Test Facility (FFTF), where its commercial viability was proven when exposed to a sodium environment.

The properties discussed previously, such as power level, fuel composition, coolant type, coolant fraction, etc. are selected to achieve a single goal: to precisely balance the burning of U-235 with the production of Pu-239. If accomplished, the reactor's multiplication factor, k_{eff} , is allowed to remain near its initial value throughout the lifetime of the core.

The core is designed to be relatively small, with total dimensions of a 1.9-meter height and a 2-meter diameter. These dimensions include a 15 cm-thick depleted uranium (DU) blanket surrounding the fuel region on all sides, and a 10 cm-thick nickel reflector surrounding the DU region. The core is modeled with several separate regions to keep track of fission products in each of the individual regions, because the power, neutron flux, and burnup vary as a function of the core radius. In addition to radial sections, the model is also divided into an equal number of vertical sections. Therefore, Figure 12 displays three radial fuel regions, each with three vertical regions, for a total of nine fueled core sections. The model's 2-D cross-sectional reactor geometry is depicted in Figure 12, and a 3-D rendering is presented Figure 13. Observe that the inner regions containing metal fuel are divided into equal volume, rather than equal radii, sections.

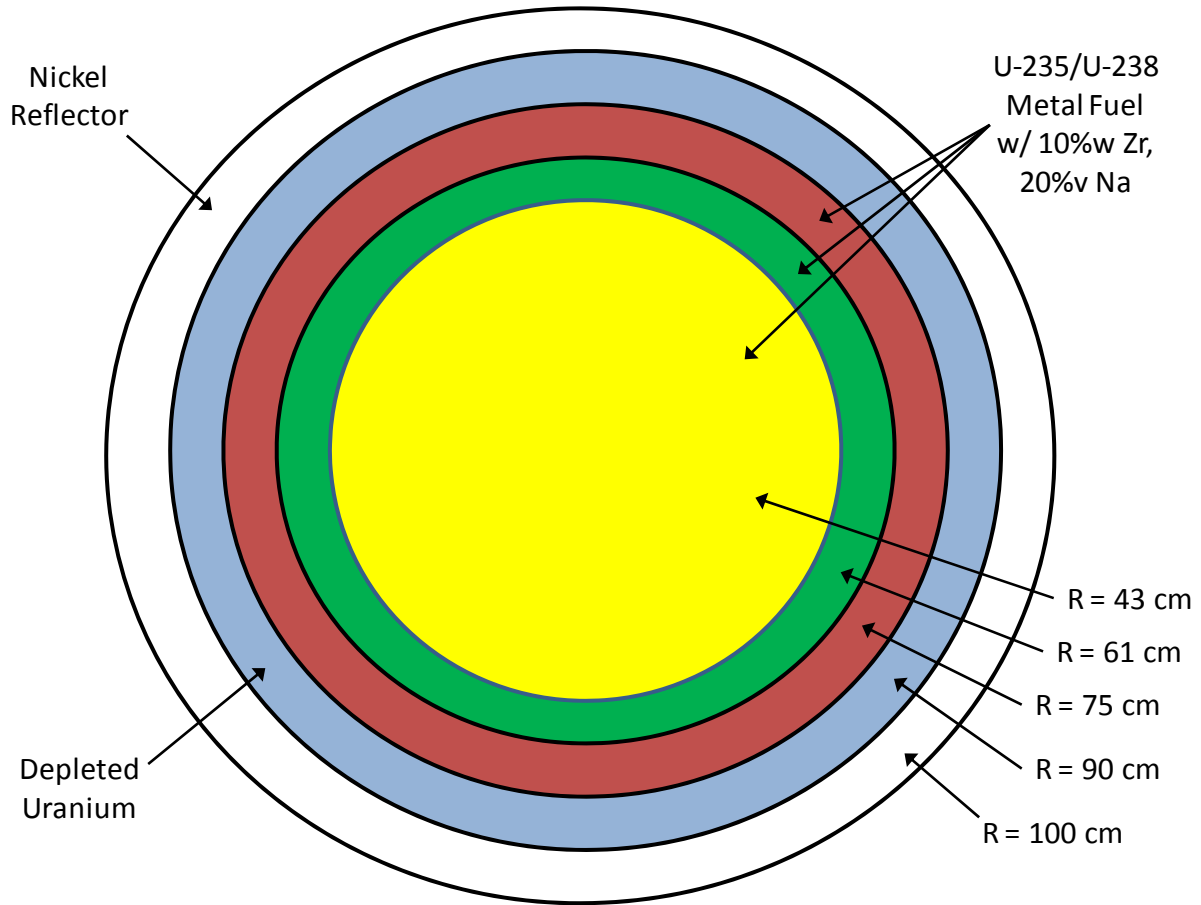


Figure 12. 2-D image of LLFR geometry used for k_{eff} calculations

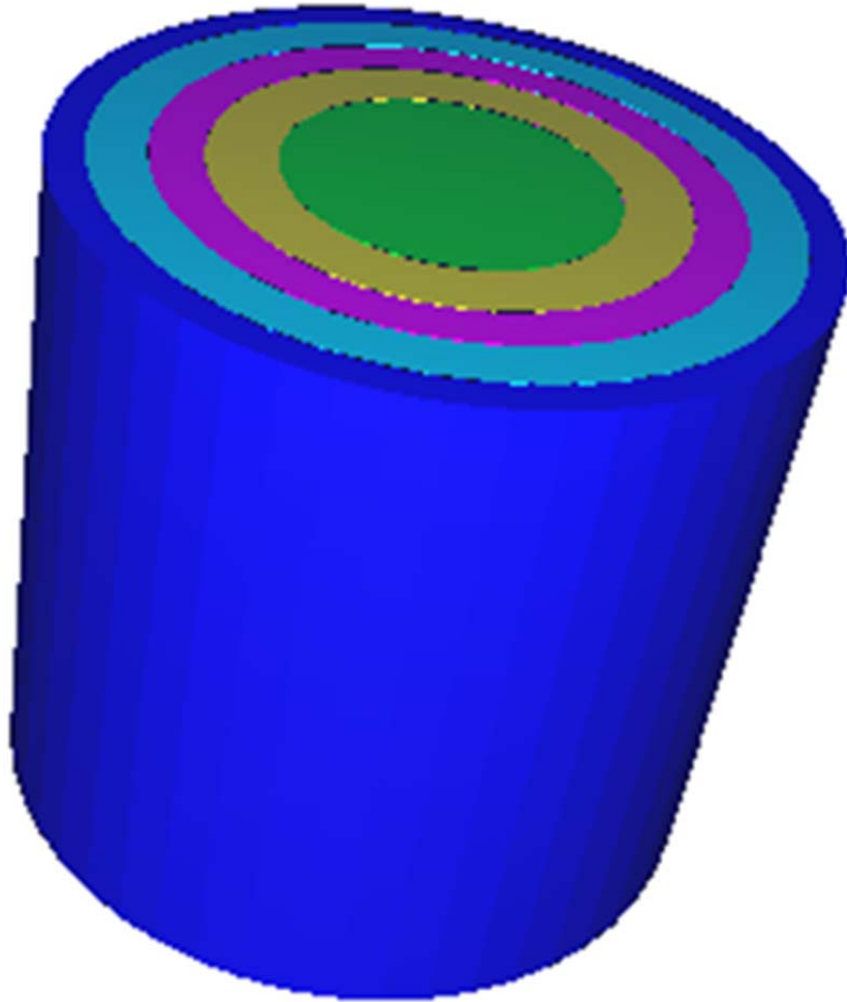


Figure 13. 3-D image of LLFR geometry used for k_{eff} calculations

The design of the core creates a hexagonal pin geometry within each region, except for the nickel reflector, which is modeled as a solid mass.

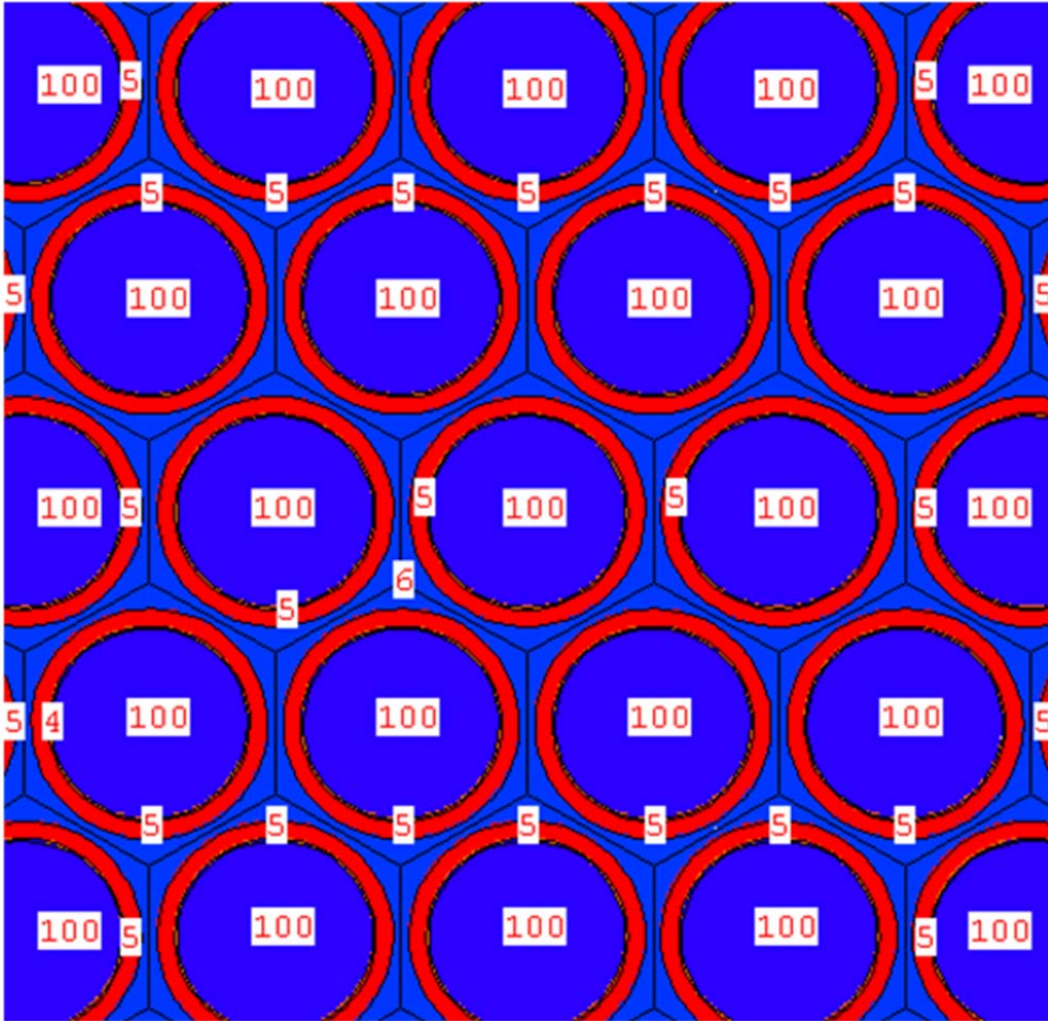


Figure 14. Pin geometry for reactor model.

The pin geometry for the LLFR concept reactor is shown in Figure 14. Cell number 100 represents fuel in the center of the fuel rods, while cells number 5 and number 6 represent cladding and coolant, respectively. There is a small, voided gap, denoted by cell number 4, between the volumes of cell 100 and cell 5 to allow for thermal expansion of the fuel, as would occur in real-world scenarios.

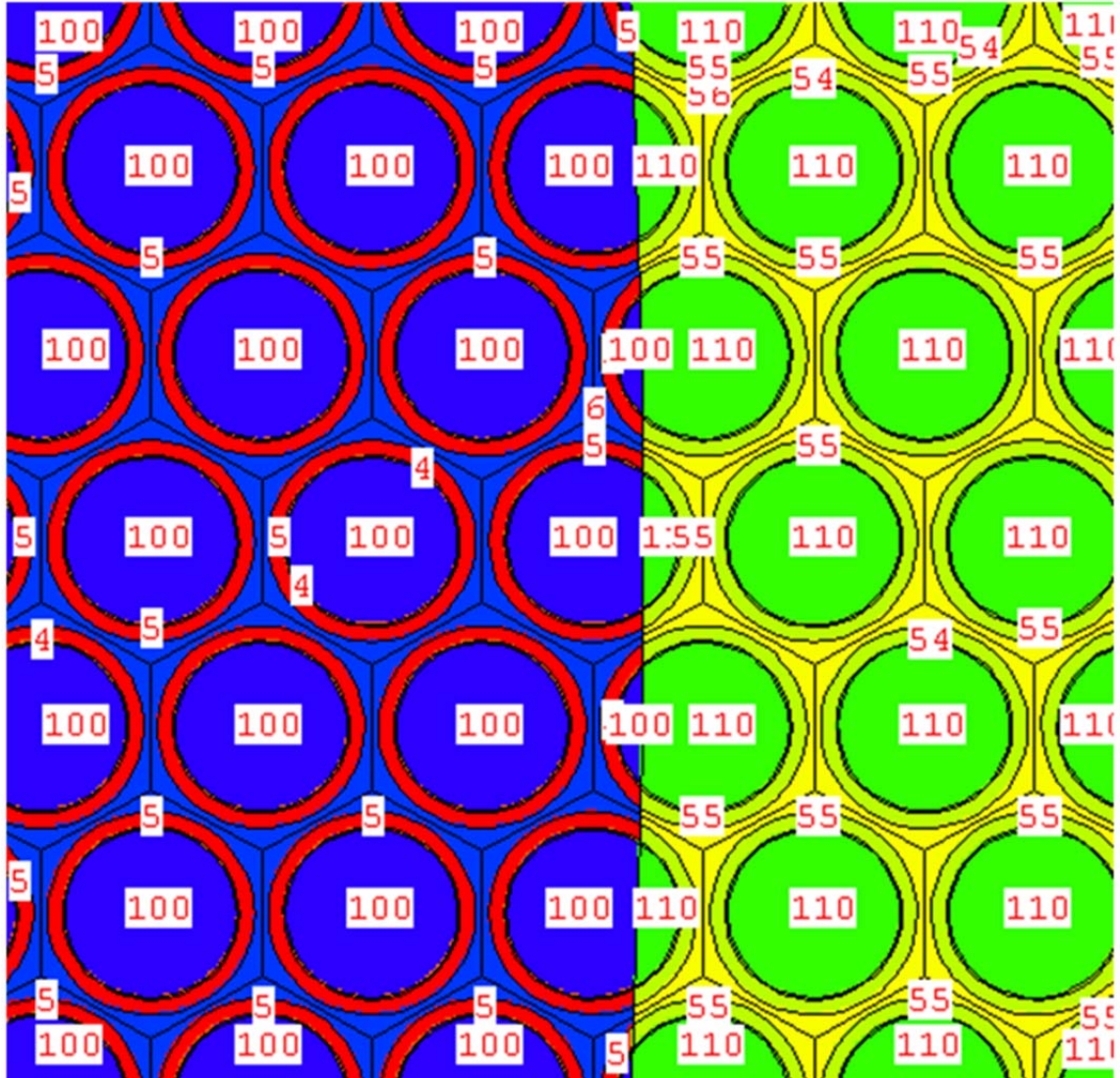


Figure 15. Core pin geometry at the boundary of two fuel regions.

The boundary between subsequent regions of fuel within the core is depicted in Figure 15. As stated previously, this is done to differentiate the burnup and concentration of fission and transmutation products. It should be observed that, due to the scoping nature of this analysis, fuel rods that lie on the boundary of the fuel regions are cut within the fuel pin. It was assumed that this would not make a decipherable difference in the analysis results. The nomenclature for Figure 15 for the region on the left is the same as denoted for Figure 14, and the region on the right follows a similar format.

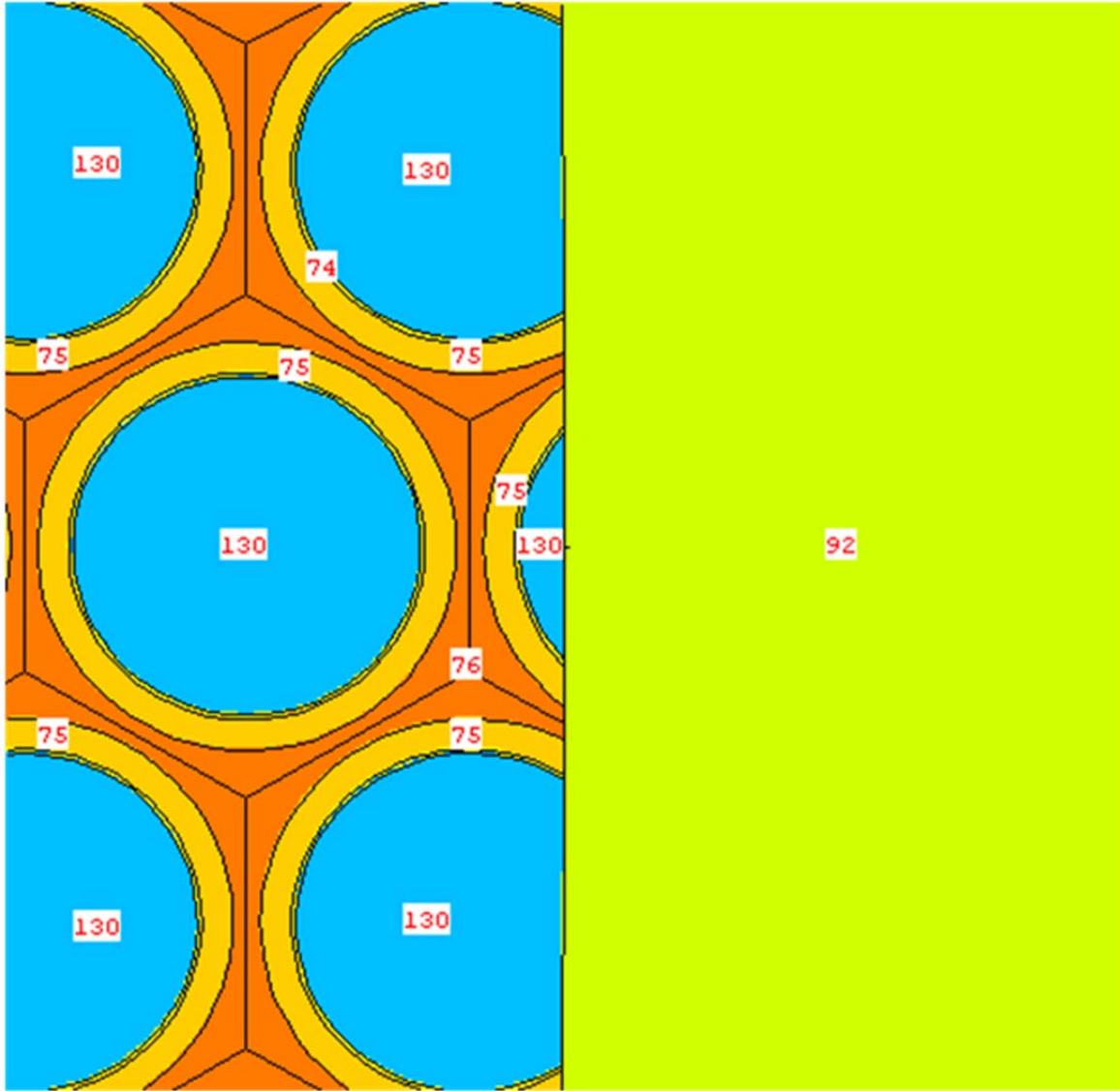


Figure 16. Core pin geometry at the boundary between the blanket region and the reflector region.

Because the nickel reflector outside the core is not created out of pins, and is modeled as a solid mass, the fuel pins that are on the boundary between the DU blanket and nickel reflector regions are cut along the region boundary, causing a fraction of a fuel pin to exist. Once again, this geometric simplification was deemed insignificant for the results of this scoping analysis. Figure 16 illustrates this situation.

4.2 Initial Results for MCNPX k_{eff} Calculations for the LLFR Reactor Concept

Figure 17 shows the MCNPX burnup results for this core design, with the case operated at 400 MW_{th} for 20 years.

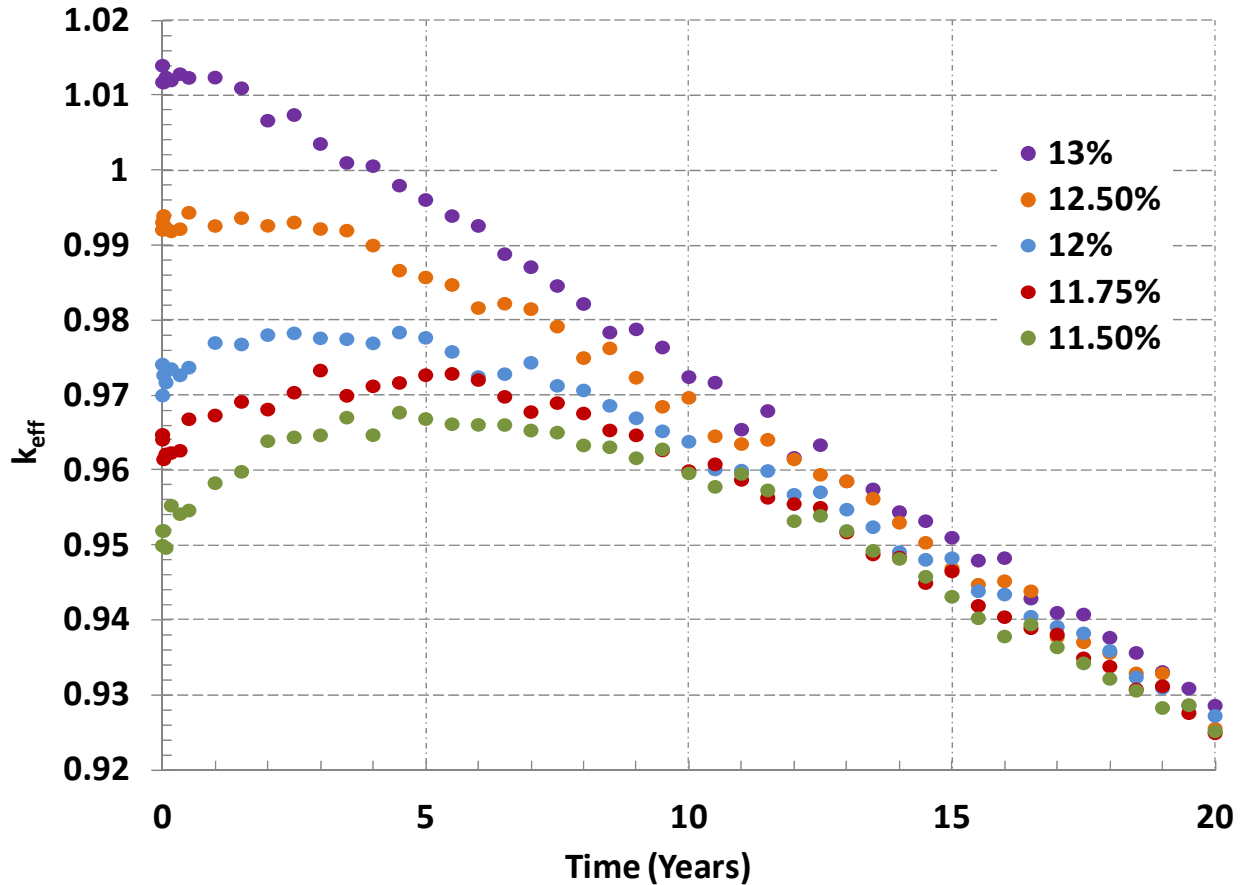


Figure 17. Results for k_{eff} using metal fuel, HT-9 cladding, and 20% cf operated for 20 years.

Based on the objectives of the LLFR concept, the most likely enrichment candidates for a prototype reactor would be 11.75% or 12%, as depicted in Figure 17. Figure 18 provides a more detailed version of Figure 17 due to lack of steady k_{eff} values past ~10 years.

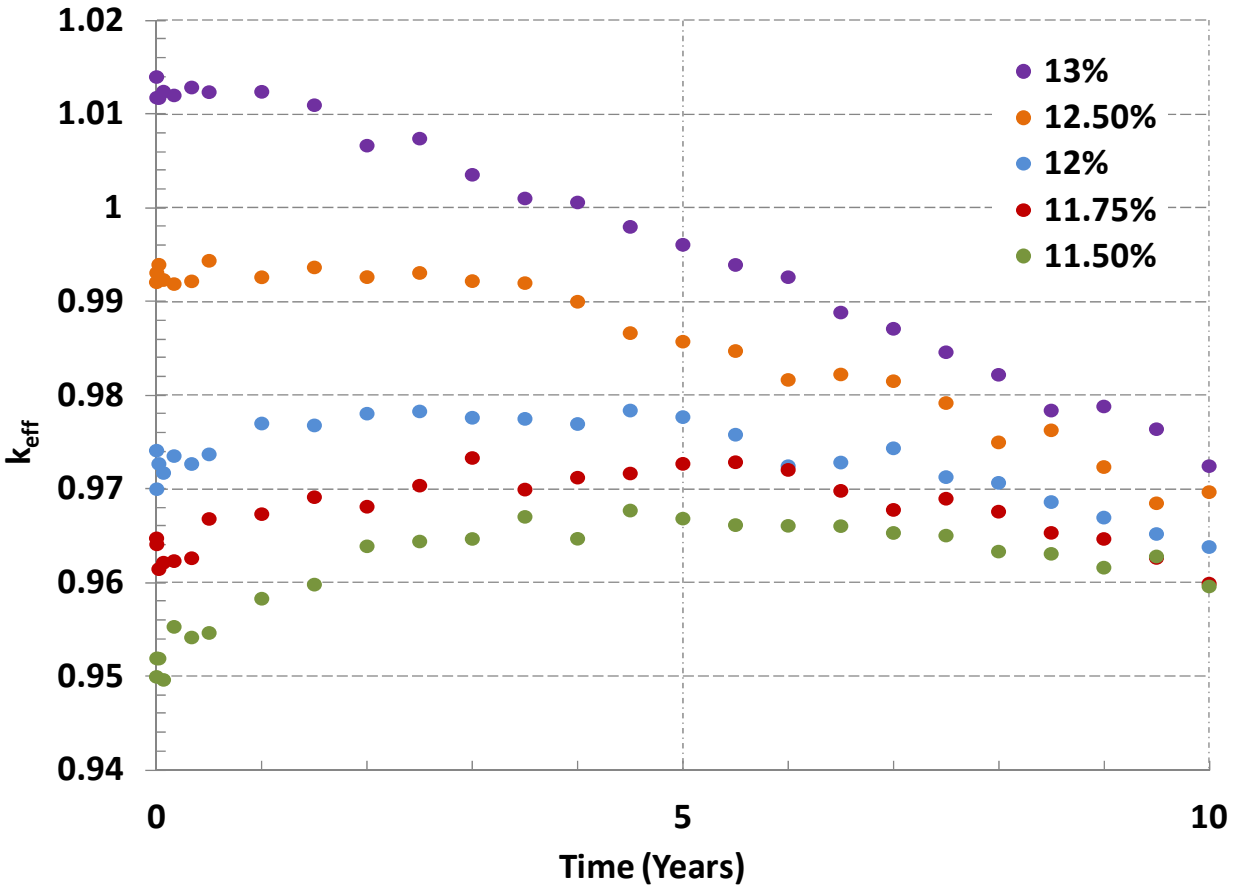


Figure 18. Results for k_{eff} using metal fuel, HT-9 cladding, and 20% cf operated for 10 years.

The results in Figure 18 provide data that confirm the LLFR concept. By designing a reactor core with the proper initial enrichment and amount of fertile material, the system maintains a relatively constant k_{eff} throughout the lifetime of the reactor. Examining Figure 18, it is clear that some values of enrichment are more suited to this conceptual design than others. For example, 13% decreases consistently for the first ten years of core lifetime, while 11.75% initially rises, then returns to its approximate BOL value.

The LLFR concept attempts to balance the usage of U-235 fissionable material with the production of fissionable Pu-239 through the transmutation of U-238. However, as this transition occurs from one fuel type to another, several reactor parameters are altered, such as β_{eff} , whose transition is illustrated in Figure 19, which confirms the transition of dominant fuel from uranium to plutonium. The β_{eff} at BOL is ~ 0.00725 , a typical value for a U-235 fueled reactor with a fast neutron spectrum. The β_{eff} value then decreases to an end of life (EOL) value of ~ 0.00375 , a proper figure considering the plutonium-dominated, mixed-fuel core. The values were obtained by running individual MCNP5 cases using the “KOPTS” card. Material concentrations for the β_{eff} cases were taken from each time step’s results in the MCNPX case.

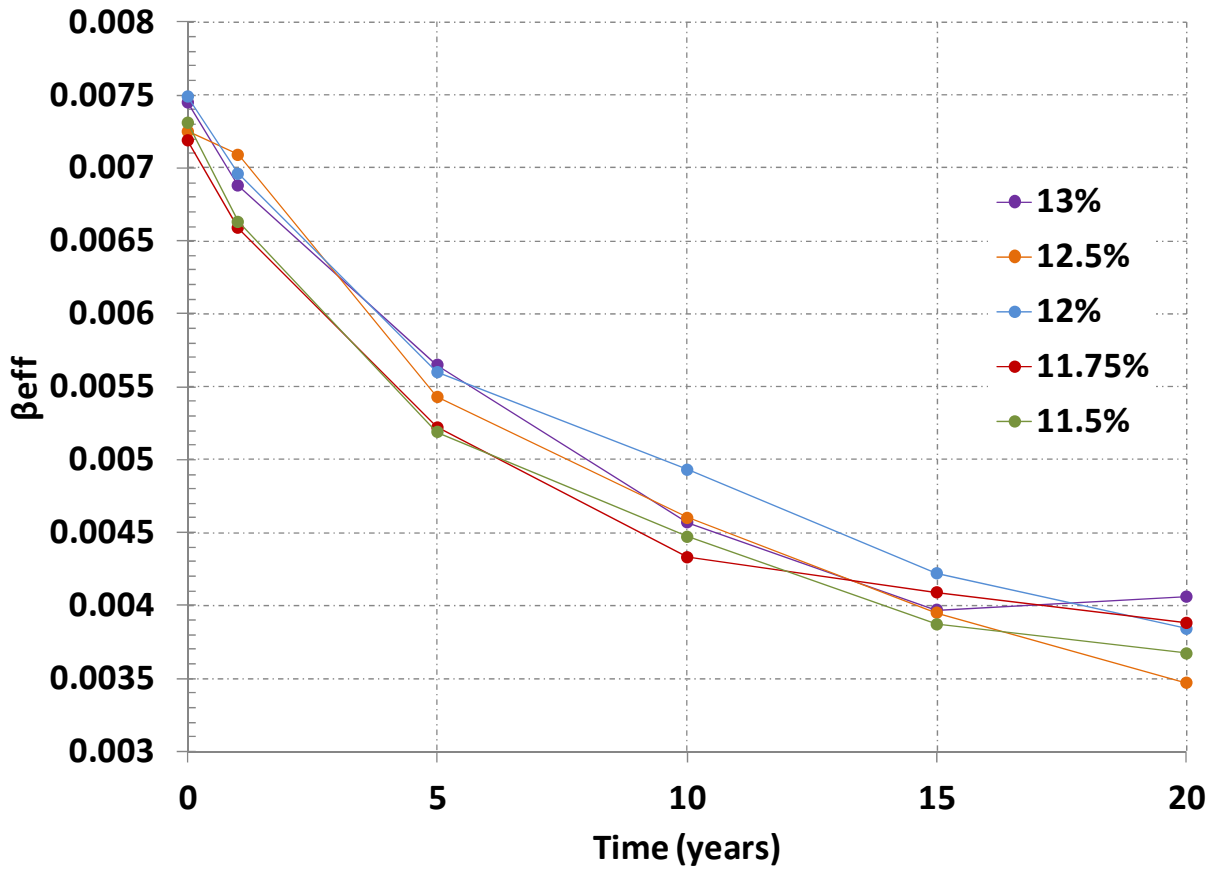


Figure 19. β_{eff} as a function of time for LLFR concept reactor

As a measure of steadiness in the multiplication factor for the given enrichment, Figure 20 displays the change in reactivity as a function of operating time for the reactor. Observe that an optimal duration of operation for the 11.75% enrichment LLFR concept is approximately 10 years, indicating that the focus should be on this enrichment and duration for future, more sensitive analyses. Figure 20 uses Figure 19 to attain β_{eff} values to calculate the change of reactivity in dollar units of reactivity.

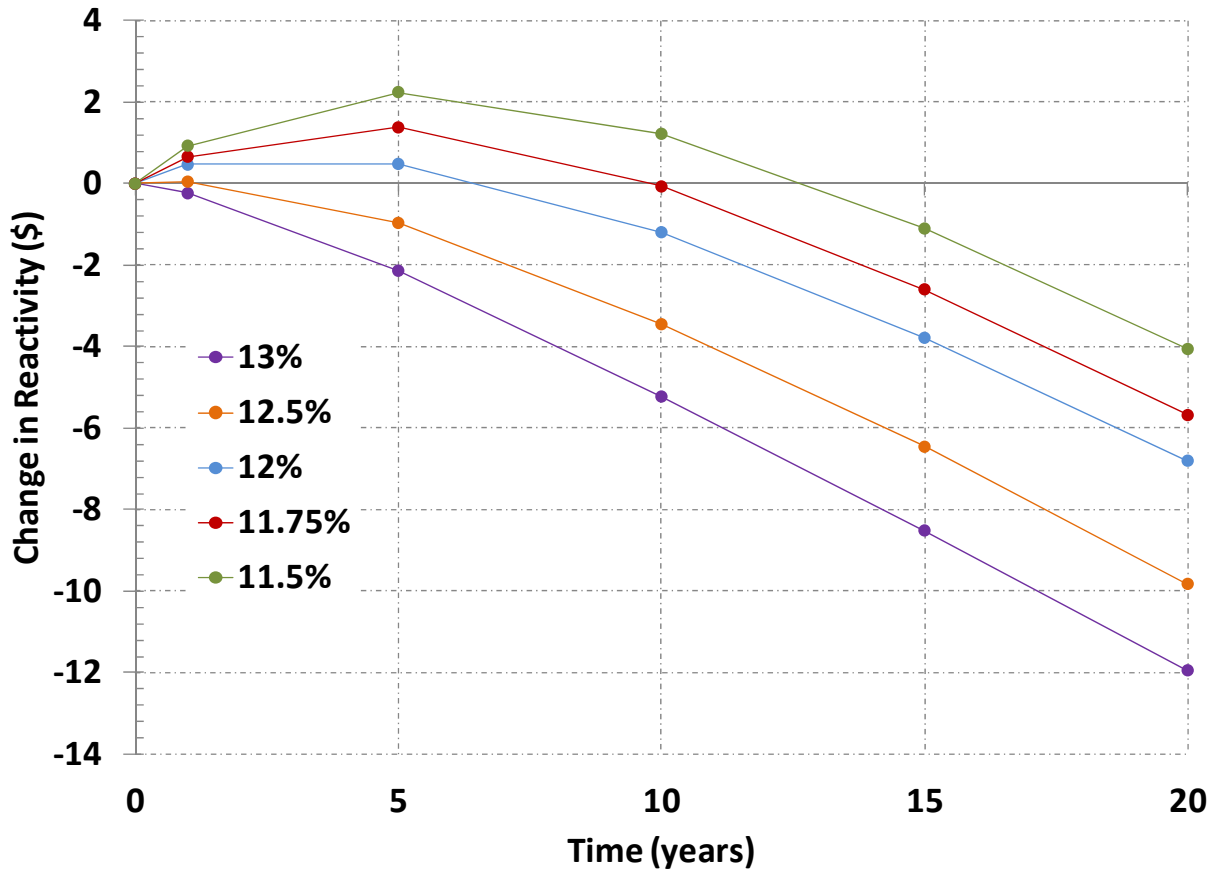


Figure 20. Change in reactivity as a function of time for LLFR concept reactor.

To provide a feasible design for a LLFR concept reactor, the void reactivity worth must be quantified. Traditionally, only reactors with a negative void coefficient are deemed sufficiently safe, though innovations in reactor safety and control render the idea of building a reactor with a positive void coefficient (such as a sodium-cooled fast reactor) more plausible. Figure 21 depicts the void reactivity worth as a function of reactor operating time. These void coefficient calculations are performed at full void conditions, although this is highly unlikely since the boiling point of liquid sodium is 1156K at atmospheric condition. At BOL, the void coefficient is negative due to the dominating presence of U-235 in comparison with any other fissionable fuel material. However, as U-235 is used up and Pu-239 becomes the driving fission source in the reactor, the void coefficient becomes positive, with the changeover occurring at approximately 2 years. This series of void coefficient calculations used a sodium coolant fraction of 20%, as discussed previously.

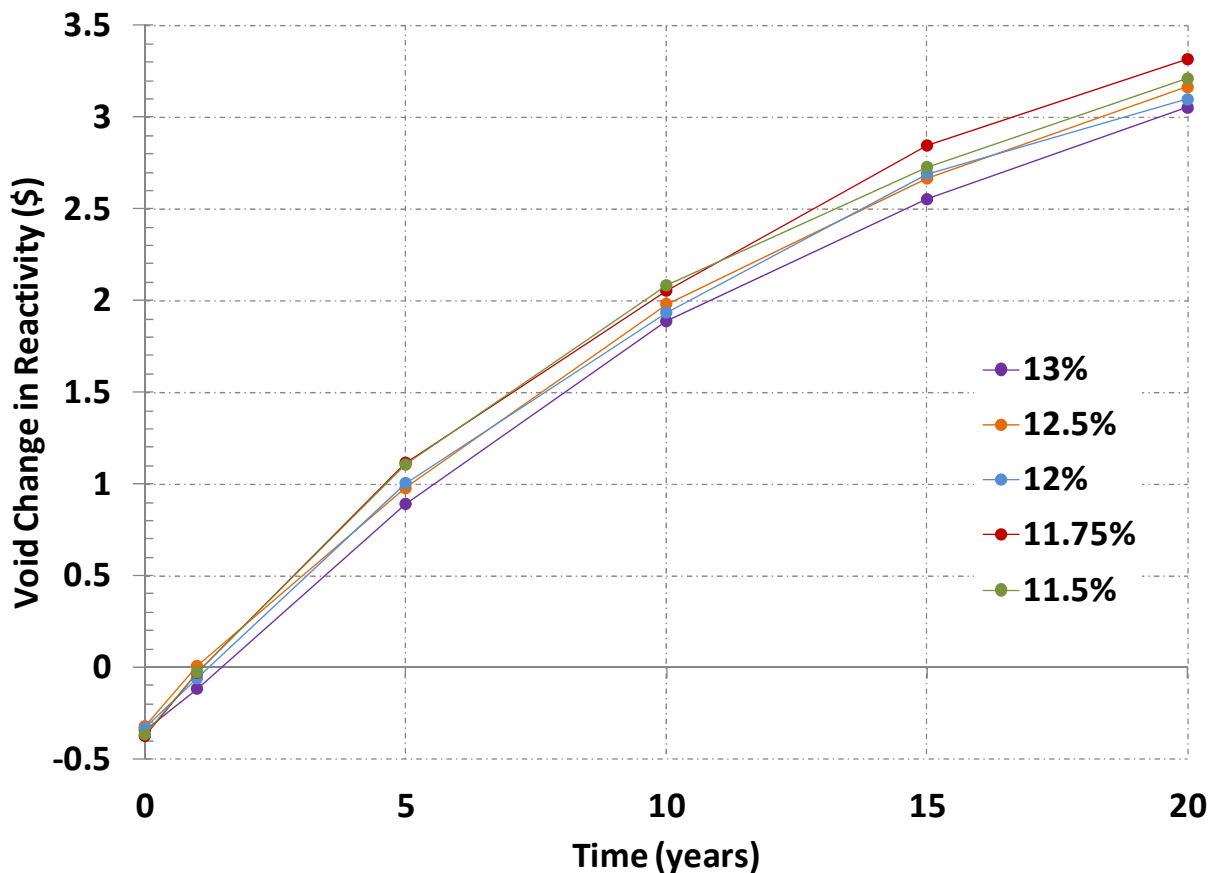


Figure 21. Void reactivity worth as a function of time for LLFR concept reactor.

The void reactivity depicted in Figure 21 is a result of burnup in the LLFR core. By voiding the core, higher energy neutrons are present. As compared to neutrons whose energy is lower due to slight moderation by the sodium coolant, Pu-239 has an increase η value. In comparison, the negative void reactivity at BOL occurs due to the decreased η value for uranium atoms if higher energy neutrons are present.

The MCNP runs that have been performed so far have used a value of 400 MW_{th} for the reactor power. However, this was chosen as an arbitrary starting point, because this power level is a reasonable figure for a reactor core that is small in size, relatively high enrichment, and medium-level core power density. For illustrative purposes, Figure 22 shows the change in the multiplication factor when the initial core enrichment (12.5% enriched from Figure 17) is run at half-power (200 MW_{th}). It can be observed that the k_{eff} for 20 years at 200 MW_{th} is almost identical to k_{eff} for 10 years at 400 MW_{th}.

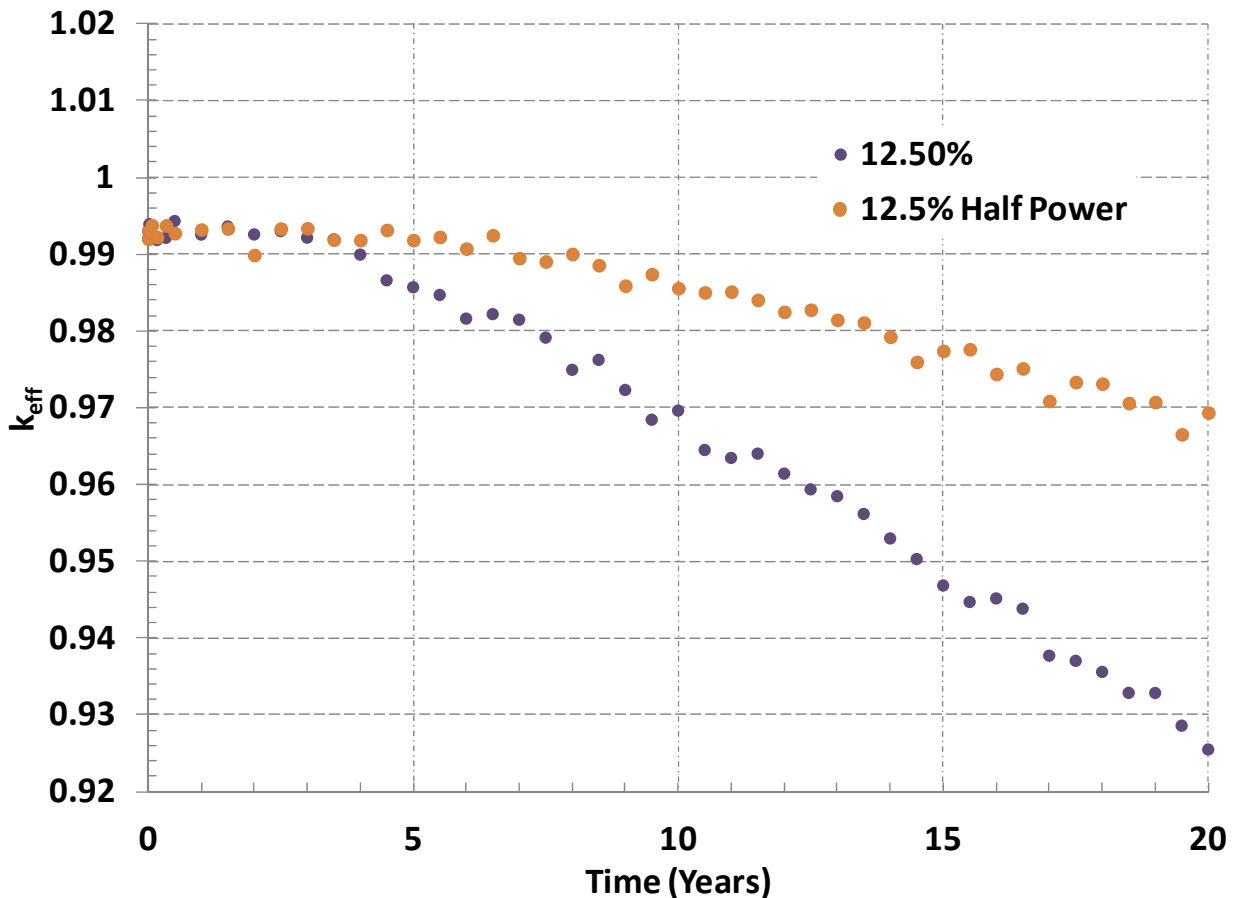


Figure 22. Comparison of relative power levels for LLFR concept reactor

Within Figure 17, the values for k_{eff} are less than one for several of the levels of enrichment for this core, but the results for 11.75% and 12% are promising, with respect to changes in reactivity over the lifetime of the core. During the burnup calculations, MCNPX ignores the subcriticality of the geometry, instead forcing the reactor to progress through a 400 MW_{th} power level during each time step. However, if this scoping analysis is to evolve into a commercial reactor design, k_{eff} must be greater than unity. Further investigation was, therefore, performed into increasing the reactor size, decreasing the fuel pitch, or increasing the width of the DU blanket and/or nickel reflector to increase k_{eff} for the LLFR concept reactor.

4.3 Core Modifications for LLFR Concept Reactor

From the initial k_{eff} calculations illustrated in Figure 17, it is estimated that an accurate timeframe for further MCNPX runs would be 10 years, ensuring that k_{eff} did not decrease too severely from its BOL value. Additional calculations were then performed, comparing the k_{eff} values using the data collected after 10 years to differentiate between the geometry modifications. The two “flattest” profiles exhibited in Figure 18 were the 11.75% and 12% enriched geometries, so these enrichments were explored with altered parameters in further MCNPX runs to determine adjustments that would result in a k_{eff} larger than one. The first notion is to increase the size of the reactor slightly by altering the diameter or the height of the core. Next, by decreasing the coolant fraction of the core, the pitch is decreased, allowing more fuel rods to be contained in a unit area, increasing k_{eff} . However, it is unknown what kind of effects this will have on thermal hydraulic analyses in the LLFR concept reactor. Finally, by increasing the width of either the DU blanket or the nickel reflector, small adjustments may be made in the multiplication factor of the reactor. Table 2 summarizes these parameter modifications and the effect they had on k_{eff} , as well as compares them to the original, referenced case. The reference case and all the parameter modification runs were operated at an 11.75% enrichment level. In Table 2, “mh” and “md” represent the height in meters and the diameter in meters, respectively.

Table 2. Parameter modifications for 11.75% enriched core

Core Parameters	k_{eff} (at EOL - 10 year)
Reference case (2mdx1.9mh, 20% cf, 15 cm DU, 10 cm Ni)	0.97259
2mdx2.1mh	0.98323
2.1mdx2.1mh	0.99436
2.1mdx1.9mh	0.98366
2.25mdx2.25mh	1.01512
2.4mdx1.9mh	1.00951
2.4mdx2.25mh	1.02718
15% cf	0.9936
17.5% cf	0.98329
25cmNi	0.98038
25cmDU	0.98017
25cmNiDU	0.9837

This design does not incorporate control rods of any kind within this analysis, in accordance with the current the scope of the work. However, it is envisioned that the core would be controlled by control rods in the core or by a movable reflector. This analysis explored control of the reactor by the adjustment of the nickel reflector. By removing or partially removing the reflector, neutron leakage increases and k_{eff} decreases adequately to allow for proper operation of the reactor. This can be shown (see Table 3) by reducing the height of the reflector to 50% and 0% of its original height.

Table 3. Reflector alterations for 11.75% enriched core

Reflector Parameter	k_{eff} (operated 10 years)
Reference case	0.97259
50% Reflector	0.95893
0% Reflector	0.95423

Using a β_{eff} value of approximately 0.004 (from Figure 19) to obtain the change in reactivity in dollar units, the negative reactivity insertion for 50% and for 100% removal of the reflector after 10 years operation is equivalent to approximately \$3.66 and \$4.95, respectively.

Because the results from Figure 17 show that the multiplication factor is less than unity, the size of the core should be increased. This is, conceptually, the simplest way to increase k_{eff} . From Figure 17, the most likely enrichment candidates to fulfill the LLFR concept objectives were 11.75% and 12%. Figure 23 indicates how k_{eff} changes when the size of the core is increased for the 12% enriched case. The reference case in Figure 23 has size dimensions that are identified in Table 2.

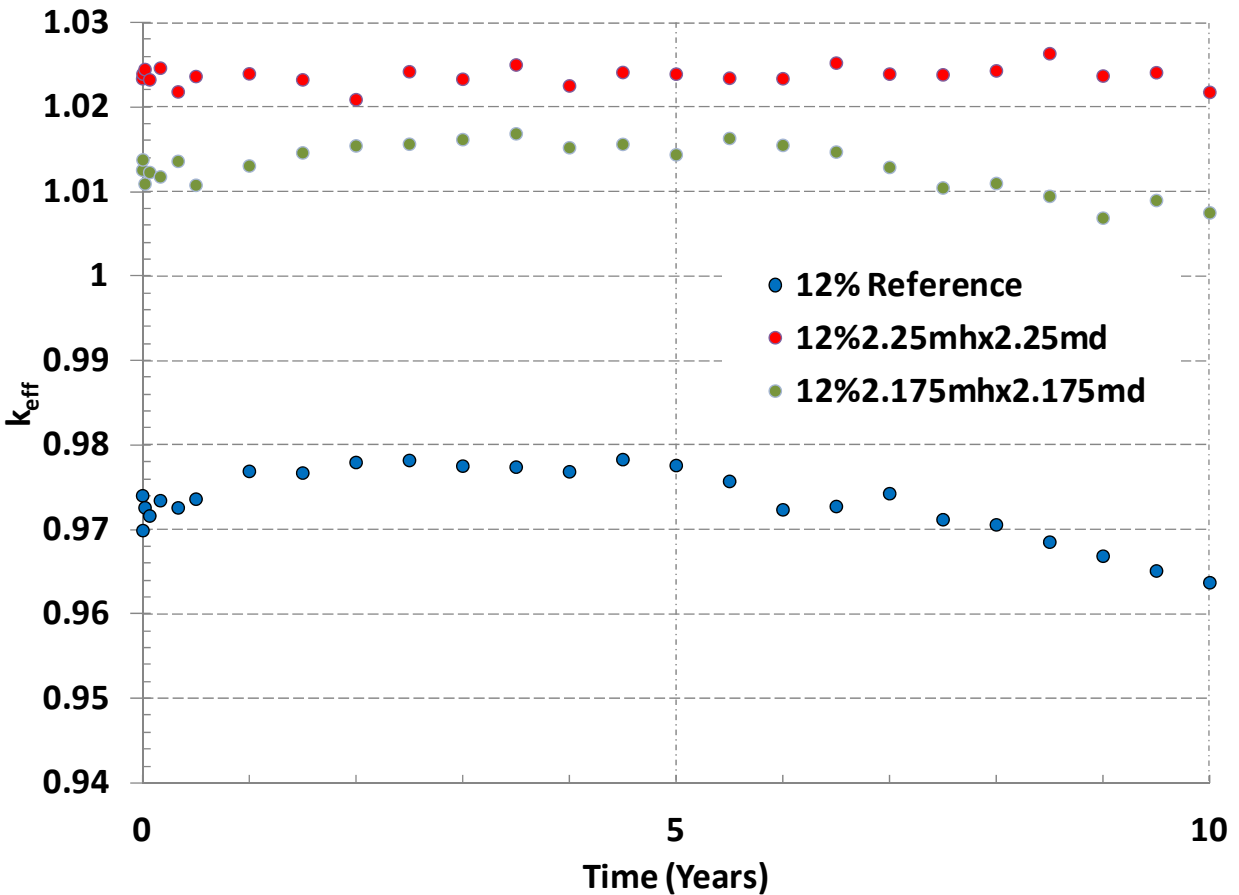


Figure 23. Core size modifications for 12% enriched LLFR concept

Figure 24 shows the effect of core size modifications for an enrichment of 11.75%. The reference case in Figure 24 has size dimensions that are identified in Table 2.

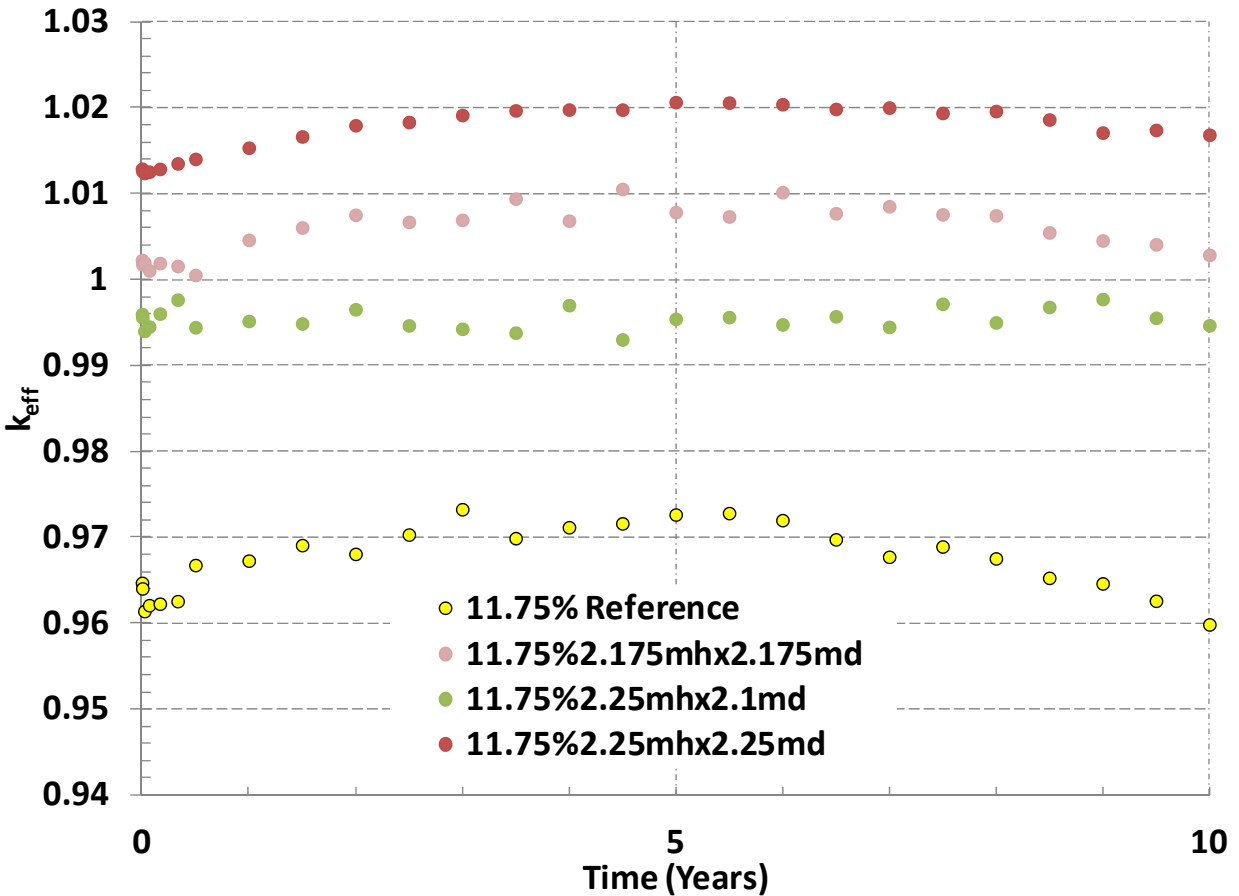


Figure 24. Core size modifications for 11.75% enriched LLFR concept.

An approximate core size of a 2.175 meter height and a 2.175 meter diameter provides a k_{eff} value above unity that stays fairly constant throughout the lifetime of the reactor for both the above enrichments. A future reactor built with the ideals of the LLFR concept will most likely exhibit these approximate diameters and enrichment, because it allows the initial reactor core to produce power for at least 10 years without zone loading, periodic fuel reshuffling, or refueling.

4.4 Coolant Modifications

A brief investigation was also done to evaluate the use of different liquid metals for cooling of the LLFR concept. Sodium provides a lesser amount of moderation when compared to using water in a traditional LWR, resulting in a faster energy spectrum. However, other liquid metals, such as lead (Pb) or lead-bismuth (PbBi), are possible coolant choices for any future reactor design. Lead and lead-bismuth both increase the average neutron energy, since the larger atoms do not provide as much moderation as the lighter sodium atoms. The same k_{eff} cases were run by MCNPX for both of these, and the results are depicted in Figure 25.

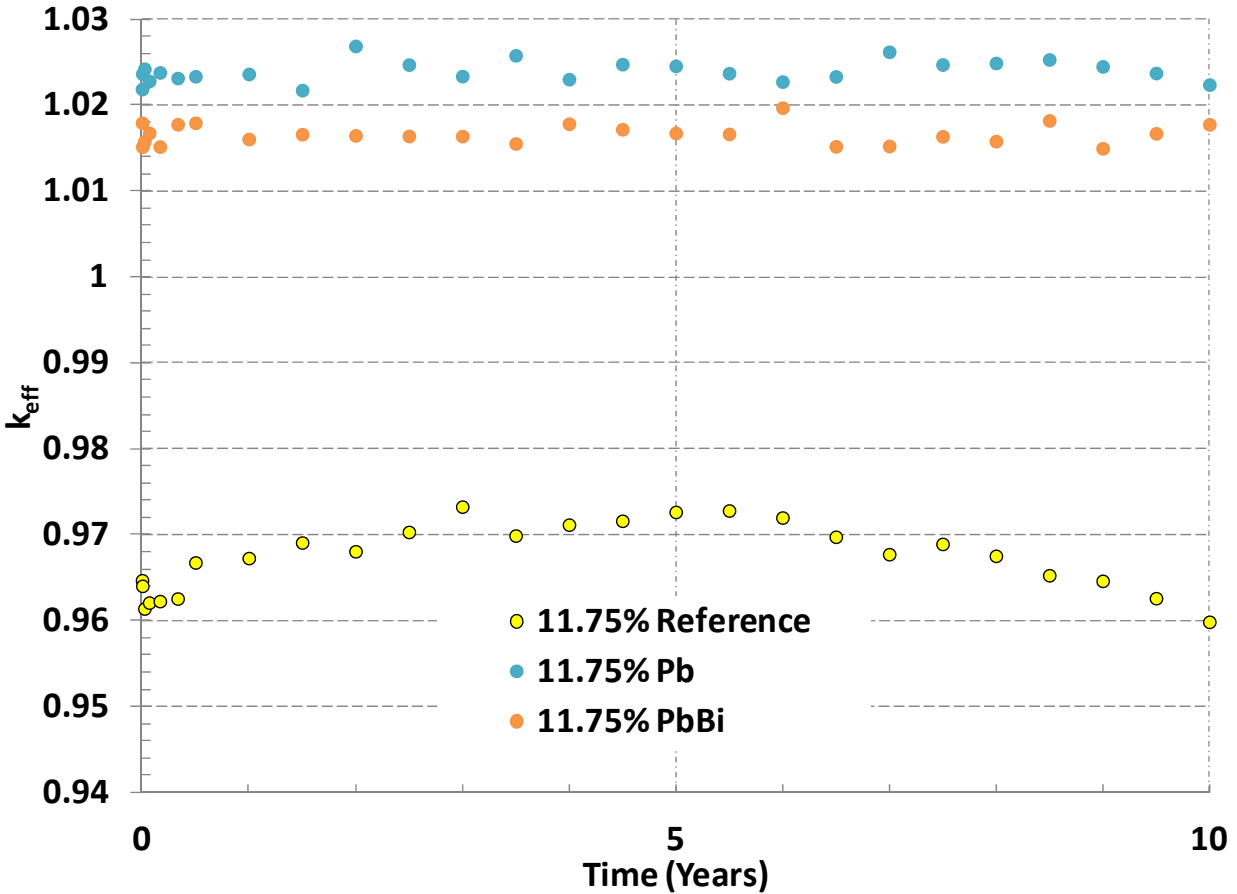


Figure 25. Coolant modifications 11.75% enriched LLFR concept reactor.

By including lead or lead-bismuth as the liquid metal coolant, the k_{eff} value is brought above one, allowing this to be a plausible LLFR concept design without increasing the core size. It also appears that both the lead and lead-bismuth cases appear to exhibit “flatter” profiles than that of the reference case. The alteration in the profile shape is most likely due to the different energy spectrum resulting from neutrons scattering off heavier atoms in the liquid metal coolant. Additionally, lead and lead-bismuth do not present the same explosive chemical hazards that are present with sodium, as well as giving the system an extremely negative void coefficient throughout the core lifetime rather than the phenomenon observed in Figure 21.

4.5 Future Generation LLFR Cores

An additional goal for this research is to be able to create a second core using material exclusively from the first core. However, by EOL, k_{eff} is less than one due to the accumulation of fission products and other non-fissioning isotopes. To obtain material for a second core, reprocessing must be performed, taking into account proliferation concerns. The concept for the LLFR at the second stage, therefore, is to only remove fission products from the fuel during reprocessing. In addition, the reprocessing should remove all uranium isotopes from the fuel material, because chemical separation will collect U-238 and U-235 into a single entity. This

semi-depleted uranium could then be put to use at another site or another first generation reactor core. To determine how the multiplication factor of this remaining second generation mixture would change over time, a k_{inf} case was run with MCNPX. The second generation core uses the previously-bred plutonium as the core's fissionable material. Then, by incrementally adding U-238 to the homogeneous mixture, it was determined that the k_{inf} could be adjusted to provide fertile breeding material to increase and balance the long-term core reactivity.

Figure 26 illustrates the results for the second generation core. These MCNPX cases were run using the same fuel pellet geometry described in earlier sections. In the legend of Figure 26, the U-238 ratio represents the atom fraction of U-238 added to the homogeneous mixture. As a reference, the first core k_{inf} case for an enrichment of 12% is included, since this enrichment provided a relatively flat k_{eff} profile during later analyses.

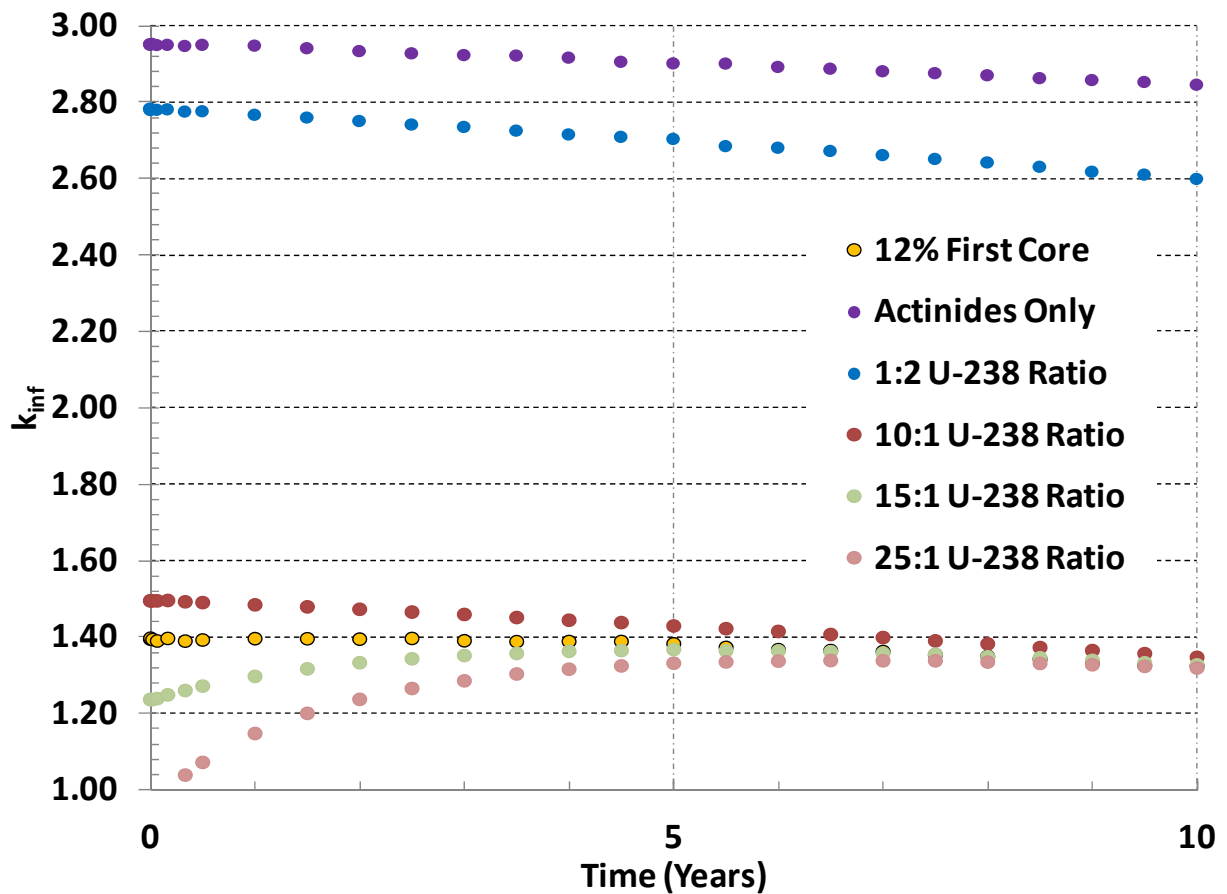


Figure 26. Results of 2nd Generation Core

Based on these results, it is plausible that a second core could be constructed from the initial core material remaining after the first 10 years of operation time. By chemical separation of uranium and fission products from the first core, the new case, composed of exclusive actinides, displays the characteristics shown by the purple dots (Actinides Only). This material is plutonium-rich, which is verified by the large k_{inf} value in Figure 26. However, its slope does not exhibit a desirable “flat” profile. The remaining k_{inf} test cases are created by adding U-238 to the

Actinides Only case. It is clear that only adding fifty atom percent of U-238 to the actinides does not provide a flat profile, though by adding enough uranium to create an approximately 13:1 ratio of uranium to actinides, a stable, flat k_{inf} profile over a span of ten years is created.

Therefore, due to the higher enrichment for the initial core compared to an LWR, the initial core would be more expensive per kg of fuel, though the small volume of an LLFR concept reactor helps to minimize this cost. However, the advantage of an LLFR concept reactor is the increased reactor lifetime, as well as the vastly reduced cost for a subsequent core, whose lifetime is approximately 10 years without zone loading or reshuffling (which is essentially equivalent to the initial core's operating characteristics).

5. CONCLUSIONS

The results of this scoping analysis were successful in providing a preliminary reactor design to continue research in this area. This LLFR concept involves metal U-235/U-238 fuel with HT-9 fuel cladding and sodium coolant. The coolant fraction will remain at 20%, equivalent to the first set of k_{eff} MCNPX runs. The enrichment for further design considerations will be 11.75%, because its effective change in reactivity over ten years is very small. However, due to the first set of k_{eff} runs possessing a multiplication factor of less than unity, the new size of the core will be an overall height of 2.175 meters, with an overall diameter of 2.175 meters.

6. FUTURE WORK

There is a substantial amount of work required to transform this conceptual idea to a full-scale commercial reactor design. In the immediate future, an array of thermal hydraulic analyses need to be performed to determine the proper coolant and fuel temperatures based on the expected flow conditions for an LLFR concept reactor. Because liquid metal coolants do not experience a phase change during reactor operation, some complications associated with LWRs can be avoided in this type of fast reactor design.

To enhance the neutronics behavior for the LLFR concept design, the core can also be divided into finer cross-sectional volumes to calculate a more accurate burnup in each region of the core, though any further analysis in this area is not expected to substantially alter any k_{eff} profile shapes or coefficient calculations throughout the life of the reactor.

Finally, during this scoping analysis for the LLFR concept, only a single fuel type was examined. In future work, traditional oxide fuels could be examined for a thorough investigation of existing reactor models. Next, more exotic fuels, such as uranium carbide (UC) or uranium nitride (UN), and advanced fuel cycles, such as thorium, may be included into the LLFR concept analyses.

7. REFERENCES

Bays, S.E., Zhang, H., Zhao, H., “The Industrial Sodium Cooled Fast Reactor,” ANFM 2009, Idaho National Laboratory, Idaho Falls, ID, April 2009.

Chang, Y.I., Finck, P.J., Grandy, C., “Advanced Burner Test Reactor: Preconceptual Design Report,” ANL-AFCI-173, Argonne National Laboratory, Argonne, IL, September 2006.

Crawford, D.C., Porter, D.L., Hayes, S.L., “Fuels for sodium-cooled fast reactors: US perspective,” Journal of Nuclear Materials, Vol. 371, p. 202-231, 2007.

DeHart, M.D., Zhang, H., Shaber, E., “A Study of Fast Reactor Fuel Transmutation in a Candidate Dispersion Fuel Design,” INL/CON-10-19000, Idaho National Laboratory, Idaho Falls, ID, November 2010.

Greenspan, E., STAR: The Secure Transportable Autonomous Reactor System: Final Report. New England Research Institutes (NERI) Project No. 99-154, University of California, Berkeley, CA, October 2003.

Kim, T.K., Taiwo, T.A., “Systematic Evaluation of Uranium Utilization in Nuclear Systems” 11th Information Exchange Meeting on Actinide and Product Partitioning and Transmutation, San Francisco, CA, November 2010.

Klueh, R.L., Harries, D.R., “MONO3: High-Chromium Ferritic and Martenitic Steels for Nuclear Applications, Chapter 2: Development of High (7-12%) Chromium Martenitic Steels,” West Conshohocken, PA, 2001.

MCNP – A General Monte Carlo N-Particle Transport Code, Version 5, LA-UR-03-1987, Los Alamos, NM, April 2003.

MCNPX User’s Manual, Version 2.7.0, LA-CP-11-00438, Los Alamos, NM, April 2011.

NuDat 2.6. Alejandro Sonzogni. Brookhaven National Laboratory & National Nuclear Data Center. 1 December 2012. <<http://www.nndc.bnl.gov/nudat2/>>

Parma, E.J., Advanced Nuclear Concepts Division 6221, “BURNCAL: A Nuclear Reactor Burnup Code Using MCNP Tallies”, SAND2002-3868, Sandia National Laboratories, Albuquerque, NM, November 2002.

Parma, E.J., Wright, S.A., Vernon, M.E., Fleming, D.D., Rochau, G.E., Suo-Antilla, A.J., Rashdan, A.A., Tsvetkov, P.V., “Supercritical CO₂ Direct Cycle Gas Fast Reactor (SC-GFR) Concept,” SAND2011-2525, Sandia National Laboratories, Albuquerque, NM, May 2011.

Walters, L., Lambert, J., Natesan, K., Wright, A., Yacout, A., Hayes, S., Porter, D., Garner, F., Ott, L., Denman, M., “Sodium Fast Reactor Fuels and Materials: Research Needs,” SAND2011-6546, Sandia National Laboratories, Albuquerque, NM, September 2011.

THIS PAGE INTENTIONALLY LEFT BLANK.

APPENDIX A – SAMPLE INPUT DECK

Long Li fe Fast Reactor

c Created June 2012
 c Thomas Hol schuh
 c tvhol sc@sandi a. gov
 c Edward Parma
 c ej parma@sandi a. gov
 c 11.75% ---> keff = 1.00 @ 10yrs
 c 2.175m Di ameter x 2.175m Hei ght

c -----
 c cell cards (80 total)
 c -----

c Fuel Gri ds

c
 10 101 -10.6 -101 5 -6 u=1 \$ fuel regi on 1
 11 102 -10.6 -101 7 -8 (-5 : 6) u=1 \$ fuel regi on 2
 12 103 -10.6 -101 9 -10 (-7 : 8) u=1 \$ fuel regi on 3
 13 104 -10.6 -101 11 -12 (-9 : 10) u=1 \$ fuel regi on 4
 14 105 -10.6 -101 13 -14 (-11 : 12) u=1 \$ fuel regi on 5
 501 50 -10.6 -101 1 -2 (-13 : 14) u=1 \$ DU regi on

c
 20 106 -10.6 -101 5 -6 u=2 \$ fuel regi on 1
 21 107 -10.6 -101 7 -8 (-5 : 6) u=2 \$ fuel regi on 2
 22 108 -10.6 -101 9 -10 (-7 : 8) u=2 \$ fuel regi on 3
 23 109 -10.6 -101 11 -12 (-9 : 10) u=2 \$ fuel regi on 4
 24 110 -10.6 -101 13 -14 (-11 : 12) u=2 \$ fuel regi on 5
 502 51 -10.6 -101 1 -2 (-13 : 14) u=2 \$ DU regi on

c
 30 111 -10.6 -101 5 -6 u=3 \$ fuel regi on 1
 31 112 -10.6 -101 7 -8 (-5 : 6) u=3 \$ fuel regi on 2
 32 113 -10.6 -101 9 -10 (-7 : 8) u=3 \$ fuel regi on 3
 33 114 -10.6 -101 11 -12 (-9 : 10) u=3 \$ fuel regi on 4
 34 115 -10.6 -101 13 -14 (-11 : 12) u=3 \$ fuel regi on 5
 503 52 -10.6 -101 1 -2 (-13 : 14) u=3 \$ DU regi on

c
 40 116 -10.6 -101 5 -6 u=4 \$ fuel regi on 1
 41 117 -10.6 -101 7 -8 (-5 : 6) u=4 \$ fuel regi on 2
 42 118 -10.6 -101 9 -10 (-7 : 8) u=4 \$ fuel regi on 3
 43 119 -10.6 -101 11 -12 (-9 : 10) u=4 \$ fuel regi on 4
 44 120 -10.6 -101 13 -14 (-11 : 12) u=4 \$ fuel regi on 5
 504 53 -10.6 -101 1 -2 (-13 : 14) u=4 \$ DU regi on

c
 50 121 -10.6 -101 5 -6 u=5 \$ fuel regi on 1
 51 122 -10.6 -101 7 -8 (-5 : 6) u=5 \$ fuel regi on 2
 52 123 -10.6 -101 9 -10 (-7 : 8) u=5 \$ fuel regi on 3
 53 124 -10.6 -101 11 -12 (-9 : 10) u=5 \$ fuel regi on 4
 54 125 -10.6 -101 13 -14 (-11 : 12) u=5 \$ fuel regi on 5
 505 54 -10.6 -101 1 -2 (-13 : 14) u=5 \$ DU regi on

c
 506 55 -10.6 -101 5 -6 u=6 \$ fuel regi on 1
 507 56 -10.6 -101 7 -8 (-5 : 6) u=6 \$ fuel regi on 2
 508 57 -10.6 -101 9 -10 (-7 : 8) u=6 \$ fuel regi on 3
 509 58 -10.6 -101 11 -12 (-9 : 10) u=6 \$ fuel regi on 4
 510 59 -10.6 -101 13 -14 (-11 : 12) u=6 \$ fuel regi on 5
 511 60 -10.6 -101 1 -2 (-13 : 14) u=6 \$ DU regi on

c Refl ector and Cool ant

c
 601 15 -8.9 -102 -1 3 u=1 \$ Ni ckel Refl ector

```

602 15 -8.9 -102 2 -4 u=1 $ Nickel Reflector
603 0 -102 101 1 -2 u=1 $ Gap
604 5 -7.9 -103 102 3 -4 u=1 $ HT-9 Cl adding
605 4 -0.97 103 3 -4 u=1 $ Sodium Coolant
C
606 15 -8.9 -102 -1 3 u=2 $ Nickel Reflector
607 15 -8.9 -102 2 -4 u=2 $ Nickel Reflector
608 0 -102 101 1 -2 u=2 $ Gap
609 5 -7.9 -103 102 3 -4 u=2 $ HT-9 Cl adding
610 4 -0.97 103 3 -4 u=2 $ Sodium Coolant
C
611 15 -8.9 -102 -1 3 u=3 $ Nickel Reflector
612 15 -8.9 -102 2 -4 u=3 $ Nickel Reflector
613 0 -102 101 1 -2 u=3 $ Gap
614 5 -7.9 -103 102 3 -4 u=3 $ HT-9 Cl adding
615 4 -0.97 103 3 -4 u=3 $ Sodium Coolant
C
616 15 -8.9 -102 -1 3 u=4 $ Nickel Reflector
617 15 -8.9 -102 2 -4 u=4 $ Nickel Reflector
618 0 -102 101 1 -2 u=4 $ Gap
619 5 -7.9 -103 102 3 -4 u=4 $ HT-9 Cl adding
620 4 -0.97 103 3 -4 u=4 $ Sodium Coolant
C
621 15 -8.9 -102 -1 3 u=5 $ Nickel Reflector
622 15 -8.9 -102 2 -4 u=5 $ Nickel Reflector
623 0 -102 101 1 -2 u=5 $ Gap
624 5 -7.9 -103 102 3 -4 u=5 $ HT-9 Cl adding
625 4 -0.97 103 3 -4 u=5 $ Sodium Coolant
C
626 15 -8.9 -102 -1 3 u=6 $ Nickel Reflector
627 15 -8.9 -102 2 -4 u=6 $ Nickel Reflector
628 0 -102 101 1 -2 u=6 $ Gap
629 5 -7.9 -103 102 3 -4 u=6 $ HT-9 Cl adding
630 4 -0.97 103 3 -4 u=6 $ Sodium Coolant
C
C Create Array of 401 elements
C
701 0 -51 3 -4 fill=11
801 4 -0.97 -201 202 -203 204 -205 206 u=11 lat=2
fill=-200:200 -200:200 0:0
1 160800r
C
702 0 -52 51 3 -4 fill=12
802 4 -0.97 -201 202 -203 204 -205 206 u=12 lat=2
fill=-200:200 -200:200 0:0
2 160800r
C
703 0 -53 52 3 -4 fill=13
803 4 -0.97 -201 202 -203 204 -205 206 u=13 lat=2
fill=-200:200 -200:200 0:0
3 160800r
C
704 0 -54 53 3 -4 fill=14
804 4 -0.97 -201 202 -203 204 -205 206 u=14 lat=2
fill=-200:200 -200:200 0:0
4 160800r
C
705 0 -55 54 3 -4 fill=15
805 4 -0.97 -201 202 -203 204 -205 206 u=15 lat=2
fill=-200:200 -200:200 0:0
5 160800r
C
706 0 -61 55 3 -4 fill=16
806 4 -0.97 -201 202 -203 204 -205 206 u=16 lat=2

```

```

          fill=-200:200 -200:200 0:0
        6 160800r
C
C 2 15 -8.9 -62 61 3 -4 $ Outside Nickel Reflector
C
C 1 0 62 :-3 :4 $ External Void
C
C -----
C surface cards
C -----
C
C 1 pz -98.75 $ Bottom of DU
C 2 pz 98.75 $ Top of DU
C
C 3 pz -108.75 $ Bottom of Nickel Reflector
C 4 pz 108.75 $ Top of Nickel Reflector
C
C Axial Fuel Regions
C
C 5 pz -16.75 $ Bottom Region 1
C 6 pz 16.75 $ Top Region 1
C
C 7 pz -33.5 $ Bottom Region 2
C 8 pz 33.5 $ Top Region 2
C
C 9 pz -50.25 $ Bottom Region 3
C 10 pz 50.25 $ Top Region 3
C
C 11 pz -67 $ Bottom Region 4
C 12 pz 67 $ Top Region 4
C
C 13 pz -83.75 $ Bottom Region 5
C 14 pz 83.75 $ Top Region 5
C
C Radial Fuel Regions
C
C 51 cz 37.4541 $ Radial 1
C 52 cz 52.9682 $ Radial 2
C 53 cz 64.8725 $ Radial 3
C 54 cz 74.9083 $ Radial 4
C 55 cz 83.75 $ Radial 5
C
C 61 cz 98.75 $ Radial DU
C 62 cz 108.75 $ Nickel Reflector
C
C Fuel Element
C
C 101 cz 0.311 $ Outer Radius of Fuel
C 102 cz 0.319 $ Gap 0.008 cm
C 103 cz 0.375 $ Cladding 0.056 cm thick
C
C 20% cf with fuel pin diameter of 0.75 cm
C 201 px 0.39925
C 202 px -0.39925
C 203 p 1 1.73205058076 0 0.7985
C 204 p 1 1.73205058076 0 -0.7985
C 205 p -1 1.73205058076 0 0.7985
C 206 p -1 1.73205058076 0 -0.7985
C
C BURN TIME= 1, 7, 16, 36, 60, 60, 180,
          180, 180, 180, 180, 180, 180, 180, 180, 180, 180,

```

180, 180, 180, 180, 180, 180, 180, 180, 180, 180, 180
 POWER= 400. 0
 MAT= 101, 102, 103, 104, 105, 106, 107, 108, 109, 110,
 111, 112, 113, 114, 115, 116, 117, 118, 119, 120,
 121, 122, 123, 124, 125, 50, 51, 52, 53, 54, 55,
 56, 57, 58, 59, 60
 AFMIN= 1. 0E-20 1. 0E-20
 PFRAC= 1. 0 26r
 BOPT= 1. 0 21 0

```

C
C -----
C material cards
C -----
C
C Fuel Density = 10. 6 g/cc
C Fuel Enrichment = 11. 75%
C 293K = 70c
C 600K = 71c
C 900K = 72c
C 1200K = 73c
C 2500K = 74c
C 60c, 66c both at 293K. 66c is newer.
C
m101 40000. 66c      -1. 06  $ Fuel
      92238. 73c      -8. 41559
      92235. 73c      -1. 12049
      92234. 73c      -0. 00196
      92236. 73c      -0. 00196
      94243. 73c      -1E-36
m102 40000. 66c      -1. 06  $ Fuel
      92238. 73c      -8. 41559
      92235. 73c      -1. 12049
      92234. 73c      -0. 00196
      92236. 73c      -0. 00196
      94243. 73c      -1E-36
m103 40000. 66c      -1. 06  $ Fuel
      92238. 73c      -8. 41559
      92235. 73c      -1. 12049
      92234. 73c      -0. 00196
      92236. 73c      -0. 00196
      94243. 73c      -1E-36
m104 40000. 66c      -1. 06  $ Fuel
      92238. 73c      -8. 41559
      92235. 73c      -1. 12049
      92234. 73c      -0. 00196
      92236. 73c      -0. 00196
      94243. 73c      -1E-36
m105 40000. 66c      -1. 06  $ Fuel
      92238. 73c      -8. 41559
      92235. 73c      -1. 12049
      92234. 73c      -0. 00196
      92236. 73c      -0. 00196
      94243. 73c      -1E-36
m106 40000. 66c      -1. 06  $ Fuel
      92238. 73c      -8. 41559
      92235. 73c      -1. 12049
      92234. 73c      -0. 00196
      92236. 73c      -0. 00196
      94243. 73c      -1E-36
m107 40000. 66c      -1. 06  $ Fuel
      92238. 73c      -8. 41559
      92235. 73c      -1. 12049
      92234. 73c      -0. 00196
      92236. 73c      -0. 00196
  
```

	94243.73c	-1E-36	
m108	40000.66c	-1.06	\$ Fuel
	92238.73c	-8.41559	
	92235.73c	-1.12049	
	92234.73c	-0.00196	
	92236.73c	-0.00196	
	94243.73c	-1E-36	
m109	40000.66c	-1.06	\$ Fuel
	92238.73c	-8.41559	
	92235.73c	-1.12049	
	92234.73c	-0.00196	
	92236.73c	-0.00196	
	94243.73c	-1E-36	
m110	40000.66c	-1.06	\$ Fuel
	92238.73c	-8.41559	
	92235.73c	-1.12049	
	92234.73c	-0.00196	
	92236.73c	-0.00196	
	94243.73c	-1E-36	
m111	40000.66c	-1.06	\$ Fuel
	92238.73c	-8.41559	
	92235.73c	-1.12049	
	92234.73c	-0.00196	
	92236.73c	-0.00196	
	94243.73c	-1E-36	
m112	40000.66c	-1.06	\$ Fuel
	92238.73c	-8.41559	
	92235.73c	-1.12049	
	92234.73c	-0.00196	
	92236.73c	-0.00196	
	94243.73c	-1E-36	
m113	40000.66c	-1.06	\$ Fuel
	92238.73c	-8.41559	
	92235.73c	-1.12049	
	92234.73c	-0.00196	
	92236.73c	-0.00196	
	94243.73c	-1E-36	
m114	40000.66c	-1.06	\$ Fuel
	92238.73c	-8.41559	
	92235.73c	-1.12049	
	92234.73c	-0.00196	
	92236.73c	-0.00196	
	94243.73c	-1E-36	
m115	40000.66c	-1.06	\$ Fuel
	92238.73c	-8.41559	
	92235.73c	-1.12049	
	92234.73c	-0.00196	
	92236.73c	-0.00196	
	94243.73c	-1E-36	
m116	40000.66c	-1.06	\$ Fuel
	92238.73c	-8.41559	
	92235.73c	-1.12049	
	92234.73c	-0.00196	
	92236.73c	-0.00196	
	94243.73c	-1E-36	
m117	40000.66c	-1.06	\$ Fuel
	92238.73c	-8.41559	
	92235.73c	-1.12049	
	92234.73c	-0.00196	
	92236.73c	-0.00196	
	94243.73c	-1E-36	
m118	40000.66c	-1.06	\$ Fuel
	92238.73c	-8.41559	
	92235.73c	-1.12049	

	92234. 73c	-0. 00196	
	92236. 73c	-0. 00196	
	94243. 73c	-1E-36	
m119	40000. 66c	-1. 06	\$ Fuel
	92238. 73c	-8. 41559	
	92235. 73c	-1. 12049	
	92234. 73c	-0. 00196	
	92236. 73c	-0. 00196	
	94243. 73c	-1E-36	
m120	40000. 66c	-1. 06	\$ Fuel
	92238. 73c	-8. 41559	
	92235. 73c	-1. 12049	
	92234. 73c	-0. 00196	
	92236. 73c	-0. 00196	
	94243. 73c	-1E-36	
m121	40000. 66c	-1. 06	\$ Fuel
	92238. 73c	-8. 41559	
	92235. 73c	-1. 12049	
	92234. 73c	-0. 00196	
	92236. 73c	-0. 00196	
	94243. 73c	-1E-36	
m122	40000. 66c	-1. 06	\$ Fuel
	92238. 73c	-8. 41559	
	92235. 73c	-1. 12049	
	92234. 73c	-0. 00196	
	92236. 73c	-0. 00196	
	94243. 73c	-1E-36	
m123	40000. 66c	-1. 06	\$ Fuel
	92238. 73c	-8. 41559	
	92235. 73c	-1. 12049	
	92234. 73c	-0. 00196	
	92236. 73c	-0. 00196	
	94243. 73c	-1E-36	
m124	40000. 66c	-1. 06	\$ Fuel
	92238. 73c	-8. 41559	
	92235. 73c	-1. 12049	
	92234. 73c	-0. 00196	
	92236. 73c	-0. 00196	
	94243. 73c	-1E-36	
m125	40000. 66c	-1. 06	\$ Fuel
	92238. 73c	-8. 41559	
	92235. 73c	-1. 12049	
	92234. 73c	-0. 00196	
	92236. 73c	-0. 00196	
	94243. 73c	-1E-36	
C			
m50	40000. 66c	-1. 06	\$ Depleted Urani um
	92235. 73c	-0. 0212	
	92238. 73c	-10. 5788	
	94243. 73c	-1E-36	
m51	40000. 66c	-1. 06	\$ Depleted Urani um
	92235. 73c	-0. 0212	
	92238. 73c	-10. 5788	
	94243. 73c	-1E-36	
m52	40000. 66c	-1. 06	\$ Depleted Urani um
	92235. 73c	-0. 0212	
	92238. 73c	-10. 5788	
	94243. 73c	-1E-36	
m53	40000. 66c	-1. 06	\$ Depleted Urani um
	92235. 73c	-0. 0212	
	92238. 73c	-10. 5788	
	94243. 73c	-1E-36	
m54	40000. 66c	-1. 06	\$ Depleted Urani um
	92235. 73c	-0. 0212	

```

92238.73c      -10.5788
94243.73c      -1E-36
m55 40000.66c   -1.06   $ Depleted Urani um
92235.73c      -0.0212
92238.73c      -10.5788
94243.73c      -1E-36
m56 40000.66c   -1.06   $ Depleted Urani um
92235.73c      -0.0212
92238.73c      -10.5788
94243.73c      -1E-36
m57 40000.66c   -1.06   $ Depleted Urani um
92235.73c      -0.0212
92238.73c      -10.5788
94243.73c      -1E-36
m58 40000.66c   -1.06   $ Depleted Urani um
92235.73c      -0.0212
92238.73c      -10.5788
94243.73c      -1E-36
m59 40000.66c   -1.06   $ Depleted Urani um
92235.73c      -0.0212
92238.73c      -10.5788
94243.73c      -1E-36
m60 40000.66c   -1.06   $ Depleted Urani um
92235.73c      -0.0212
92238.73c      -10.5788
94243.73c      -1E-36
C
m15 28058.70c   0.683  $ Ni ckel  Refl ector
      28060.70c   0.261
      28061.70c   0.011
      28062.70c   0.036
      28064.70c   0.009
C
m5  26054.72c   -0.04873 $ HT-9 Fuel  Cl addi ng
      26056.72c   -0.79993
      26057.72c   -0.01863
      26058.72c   -0.00271
      24050.72c   -0.00501
      24052.72c   -0.10044
      24053.72c   -0.01161
      24054.72c   -0.00294
      42000.60c   -0.01

```

```

C
m4  11023.71c           1  $ Sod i um Cool ant
C

```

```

C
c tmp card is used for free-gas thermal treatment of cells for neutron
transport.

```

```

C Specify only if not room temperature (2.53e-08).

```

```

C -----
tmp 1.01e-07 79r
C

```

```

C Calculate volumes for the core regions.

```

```

C Fuel fraction = pi*(r^2)/(((sq3)/2)*(P^2))

```

```

C Radius of fuel element = 0.311 cm

```

```

C Pitch of fuel in core = 0.7985 cm

```

```

C ==> Fuel fraction = 0.5503

```

```

C Example: Volume of cell 101 = pi*(R^2)*h*ff = pi*(37.4541^2)*33.5*0.5503
C = 81244.30
C

```

```

vol      81244.30 81244.30 81244.30 81244.30 81244.30 72756.09
          81244.30 81244.30 81244.30 81244.30 81244.30 72756.09
          81244.30 81244.30 81244.30 81244.30 81244.30 72756.09
          81244.30 81244.30 81244.30 81244.30 81244.30 72756.09

```

```
      81244.30 81244.30 81244.30 81244.30 81244.30 72756.09
158543.46 158543.46 158543.46 158543.46 158543.46 141979.21 44j
C
imp:n 1 78r 0
mode  n
C
C
kcode 1000 1 3 250
c kcode 1000 1 3 500
c kcode 10000 1 3 500
ksrc 0 0 0 8 0 0 -1 1 0
print 10 60 100 110
prtmp 100 100 0 1
```

APPENDIX B – EOL NON-ACTINIDE ISOTOPE INVENTORY

Table 4 provides an inventory of the 25 most abundant isotopes products at the end of the first reactor core's lifetime (20 years), representing almost 70% of all the non-actinides in the core at EOL. The isotopes are listed in decreasing abundance, with relative yield defined as the isotope concentration with respect to the total amount of non-actinide isotopes. Also included in Table 4 are the thermal neutron (n,γ) cross sections and half-life for each isotope. It should be noted that these isotopes in Table 4 are not the most abundant fission products, but instead resulted from the transmutation (neutron capture or radioactive decay) of fission products. Cross sections are taken from the online Brookhaven Chart of the Nuclides (NuDat 2.6, 2012).

Table 4. Inventory of the 25 Most Abundant Isotopes at end of core lifetime.

Isotope	Relative Yield	Absorption Cross Section (barns)	Half-life
Xenon-134	3.79%	0.2649	^{134m} Xe – 290 ms ¹³⁴ Xe – > 5.8e22 y
Cesium-135	3.43%	8.663	^{135m} Cs – 53m ¹³⁵ Cs – 2.3e6 y
Ruthenium-102	3.42%	1.27	Stable
Xenon-136	3.37%	0.2607	> 2.4e21 y
Barium-138	3.21%	0.4035	Stable
Molybdenum-100	3.15%	0.1990	7.3e18 y
Molybdenum-98	3.07%	0.130	Stable
Cesium-133	2.96%	29.0	Stable
Lanthanum-139	2.94%	9.041	Stable
Cerium-140	2.81%	0.5775	Stable
Zirconium-96	2.76%	0.02285	2.35e19 y
Xenon-132	2.63%	0.4506	^{132m} Xe – 8.39 ms ¹³² Xe – Stable
Praseodymium-141	2.61%	11.5	Stable
Zirconium-94	2.57%	0.4988	Stable
Cesium-137	2.55%	0.2501	30.08 y
Cerium-142	2.52%	0.965	> 5e16 y
Molybdenum-97	2.50%	2.197	Stable
Ruthenium-101	2.43%	5.225	Stable
Zirconium-93	2.39%	0.695	1.61e6 y
Technetium-99	2.38%	22.8	^{99m} Tc – 6.0067 h ⁹⁹ Tc – 2.11e5 y
Molybdenum-95	2.37%	13.56	Stable
Rhodium-103	2.32%	145.0	^{103m} Rh – 56.114m ¹⁰³ Rh – Stable
Ruthenium-104	2.26%	0.4716	Stable
Neodymium-143	2.24%	325.2	Stable
Neodymium-144	2.22%	3.594	2.29e15 y
Sum (25 most abundant)	68.92%	--	--

THIS PAGE INTENTIONALLY LEFT BLANK.

ELECTRONIC DISTRIBUTION

pbdavie@sandia.gov	Peter B. Davies, 6200
ejbonan@sandia.gov	Tito Bonano, 6220
gerocha@sandia.gov	Gary Rochau, 6221
deames@sandia.gov	David Ames, 6221
tmconbo@sandia.gov	Tom Conboy, 6221
ddflemi@sandia.gov	Darryn Fleming, 6221
tyholsc@sandia.gov	Tommy Holschuh, 6221
rlkeith@sandia.gov	Rodney Keith, 6221
tglewis@sandia.gov	Tom Lewis, 6221
wjmarti@sandia.gov	Billy Martin, 6221
rcmoore@sandia.gov	Bob Moore, 6221
ejparma@sandia.gov	Ed Parma, 1384
rasharp@sandia.gov	Rob Sharpe, 6221
libref@sandia.gov	Technical Library, 9536

THIS PAGE INTENTIONALLY LEFT BLANK



Sandia National Laboratories